UNIVERSITAT POLITÈCNICA DE CATALUNYA
BARCELONATECH
Escola Tècnica Superior d'Enginyeria
de Telecomunicació de Barcelona

Study of the 5G NB-IoT protocol with low density LEO Constellations of nanosatellites

Master Thesis
submitted to the Faculty of the
Escola Tècnica d'Enginyeria de Telecomunicació de Barcelona
Universitat Politècnica de Catalunya
by

Pablo Ariza Merino

In partial fulfillment
of the requirements for the master in
MASTER'S DEGREE IN TELECOMUNICATIONS ENGINEERING

Advisor: Ramon Ferrùs Ferrè
Barcelona, Date 15/05/2022

Contents

List of Figures

List of Tables

Revision history and approval record

Revision	Date	Purpose
0	09/05/2022	Document creation
1	16/05/2022	Document revision

DOCUMENT DISTRIBUTION LIST

Name	email
Pablo Ariza Merino	pabloariza5@gmail.com
Ramon Ferrús Ferré	ramon.ferrus@upc.edu

Written by: Pablo Ariza Merino		Reviewed and approved by:	
Date	09/05/2022	Date	16/05/2022
Name	Pablo Ariza	Name	Ramon Ferrús
Position	Project Author	Position	Project Supervisor

Abstract

The NB-IoT protocol, specified by 3GPP, is one of most popular and widely used technology for low-power wide-area (LPWA) networks. To further strengthen the potential of this technology, 3GPP is currently developing an extension of the NB-IoT protocol for non-terrestrial networks (NTN), so that terrestrial coverage could be extended using satellite-based network deployments and reach global coverage.

The first part of this Master's Thesis focuses on the development of a MATLAB simulation software for the characterization of a NB-IoT NTN deployment scenario in terms of satellite coverage footprint (e.g. SNR distributions) and dynamics of the satellite link during a satellite pass (e.g. time evolution of the SNR and Doppler).Among the simulator inputs, there are the satellite height, the spherical geometry of the earth, the parameters associated with the satellite, such as orbit or speed, the transmission power, frequency, pathloss, etc... The simulator allows selecting the different inputs such as NTN parameters, link budget parameters or antenna type. These inputs, which are completely configurable, are used to obtain a set of outputs that allow to characterize the NB-IoT NTN scenario, such as the characterization of the satellite coverage footprint, the antenna pointing or the characterization of the satellite pass. For each characterization, the different parameters and results obtained, such as SNR heatmaps, Doppler frequency or propagation delay, are studied in more detail.

The second part of the study is aimed at evaluating the performance of the NB-IoT NTN protocol over a satellite link. For this purpose, different numerical simulations have been performed, to estimate the minimum SNR and achievable spectral efficiency of the protocol for different communication models channels (e.g. AWGN and TDL channels, frequency offsets), different protocol configurations (e.g. number of repetitions, modulation and coding schemes) as well as considering different channel estimators. The analysis has been conducted for both downlink and uplink data channels (e.g. NPDSCH and NPUSCH). Simulations of NPDSCH Block Error Rate (BLER) and NPUSCH Block Error Rate (BLER) from the MATLAB LTE toolbox, modified and adapted to non-terrestrial communications with LEO satellites, are performed.

Resumen

El protocolo NB-IoT, especificado por el 3GPP, es una de las tecnologías más populares y utilizadas para las redes low-power wide-area (LPWA). Para reforzar aún más el potencial de esta tecnología, el 3GPP está desarrollando actualmente una extensión del protocolo NB-IoT para redes no terrestres (NTN), de modo que la cobertura terrestre podría ampliarse utilizando despliegues de redes basadas en satélites y alcanzar una cobertura global.

La primera parte de esta Tesis de Máster se centra en el desarrollo de un software de simulación MATLAB para la caracterización de un escenario de despliegue de NB-IoT NTN en términos de huella de cobertura satelital (por ejemplo, distribuciones de SNR) y dinámica del enlace satelital durante un pase de satélite (por ejemplo, evolución temporal de la SNR y Doppler).Entre las entradas del simulador, se encuentran la altura del satélite, la geometría esférica de la tierra, los parámetros asociados al satélite, como la órbita o la velocidad, la potencia de transmisión, la frecuencia, las perdidas de propagación, etc. El simulador permite seleccionar las distintas entradas, como los parámetros NTN, los parámetros del link budget o el tipo de antena. Estas entradas, totalmente configurables, se utilizan para obtener un conjunto de salidas que permiten caracterizar el escenario de la NB-IoT NTN, como la caracterización de la huella de cobertura del satélite, el apuntamiento de la antena o la caracterización del paso del satélite. Para cada caracterización, se estudian con más detalle los diferentes parámetros y resultados obtenidos, como los mapas térmicos de SNR, la frecuencia Doppler o el retardo de propagación.

La segunda parte del estudio tiene como objetivo evaluar las prestaciones del protocolo NB-IoT NTN sobre un enlace satelital. Para ello, se han realizado diferentes simulaciones numéricas, con el fin de estimar la SNR mínima y la eficiencia espectral alcanzable del protocolo para diferentes modelos de canales de comunicación (por ejemplo, canales AWGN y TDL, desplazamientos de frecuencia), diferentes configuraciones del protocolo (por ejemplo, número de repeticiones, esquemas de modulación y codificación), así como considerando diferentes estimadores de canal. El análisis se ha realizado para canales de datos de enlace descendente y ascendente (por ejemplo, NPDSCH y NPUSCH). Se realizan simulaciones de la tasa de error de bloque (BLER) NPDSCH y de la tasa de error de bloque (BLER) NPUSCH de la caja de herramientas LTE de MATLAB, modificada y adaptada a las comunicaciones no terrestres con satélites LEO.

Resum

El protocol NB-IoT, especificat pel 3GPP, és una de les tecnologies més populars i utilitzades per a les xarxes de low-power wide-area (LPWA). Per reforçar encara més el potencial d'aquesta tecnologia, el 3GPP està desenvolupant actualment una extensió del protocol NB-IoT per a xarxes no terrestres (NTN), de manera que la cobertura terrestre es podria ampliar utilitzant desplegaments de xarxes basades en satèl·lits i assolir una cobertura global .

La primera part d'aquesta Tesi de Màster se centra en el desenvolupament d'un programari de simulació MATLAB per a la caracterització d'un escenari de desplegament de NB-IoT NTN en termes de petjada de cobertura satelital (per exemple, distribucions de SNR) i dinàmica del enllaç satelital durant un passi de satèl·lit (per exemple, evolució temporal de la SNR i Doppler). Entre les entrades del simulador, es troben l'alçada del satèl·lit, la geometria esfèrica de la terra, els paràmetres associats al satèl·lit, com l'òrbita o la velocitat, la potència de transmissió, la freqüència, la pèrdua de propagació, etc. El simulador permet seleccionar les diferents entrades com són els paràmetres NTN, els paràmetres del link budget o el tipus dantena. Aquestes entrades, totalment configurables, s'utilitzen per obtenir un conjunt de sortides que permeten caracteritzar l'escenari de la NB-IoT NTN, com ara la caracterització de la petjada de cobertura del satèl·lit, l'apuntament de l'antena o la caracterització del pas del satèl·lit. Per a cada caracterització, s'estudien amb més detall els diferents paràmetres i resultats obtinguts, com ara els mapes tèrmics de SNR, la freqüència Doppler o el retard de propagació.

La segona part de l'estudi té com a objectiu avaluar les prestacions del protocol NB-IoT NTN sobre un enllaç satelital. Per fer-ho, s'han realitzat diferents simulacions numèriques, per tal d'estimar la SNR mínima i l'eficiència espectral assolible del protocol per a diferents models de canals de comunicació (per exemple, canals AWGN i TDL, desplaçaments de freqüència), diferents configuracions del protocol (per exemple, nombre de repeticions, esquemes de modulació i codificació), així com considerant diferents estimadors de canal. L'anàlisi s'ha fet per a canals de dades d'enllaç descendent i ascendent (per exemple NPDSCH i NPUSCH). Es fan simulacions de la taxa d'error de bloc (BLER) NPDSCH i de la taxa d'error de bloc (BLER) NPUSCH de la caixa d'eines LTE de MATLAB, modificada i adaptada a les comunicacions no terrestres amb satèl·lits LEO.

1 Introduction

1.1 Context

The realization of connectivity solutions for Internet of Things (IoT) applications has received much attention in the last few years, both industrially and academically, because this technology will have a global impact on the interconnection of thousands of devices and objects through the network. To this end, and to satisfy the great demand for connected devices, the 3rd Generation Partnership Project (3GPP) introduced the narrowband Internet of things (NB-IoT) standard.

This protocol is at the core of 3GPP 5G specifications for realising so called massive Machine Type Communications (mMTC). Since one of the main features of this new generation is to ensure global connectivity for IoT devices throughout the earth. This is currently not possible with terrestrial infrastructure, since in many areas of the world there is no such infrastructure, to achieve this it has been considered a viable option to use connectivity via satellites. This new connectivity will allow connection of devices in remote locations and increase the range of coverage of the current network.

The 3GPP is working to standardized the Non-Terrestrial Networks (NTN). The 3GPP is currently standardizing the so-called NB-IoT NTN, which will appear in June 2022 in Release 17, the first release to contain an NTN specification for both NR and NB-IoT/LTE-M. In this research, the NB-IoT NTN scenario has been characterized and link-level simulations have been performed in order to observe the performance of the protocol.

1.2 Objectives

The main objectives of the project are:

- Learn about the capabilities of the NB-IoT protocol, as well as the different deployment modes, the physical channels and signals that it uses, e.g., single-tone, or multi-tone transmissions, frame organization, the MCS (Modulation and Coding Scheme), or the number of repetitions.
- Characterize a typical NB-IoT NTN deployment escenario. This include characterizing the satellite satellite and all its features, the antenna used, the user device. It is possible to characterize the footprint coverage of the satellite, to obtain SNR statistics. Two types of study are included, dynamic and static study, where it will be possible to characterize the direction of the antenna beam or even multibeam scenarios. The dynamic study will also characterize the Doppler effect, the propagation delay or the variability of the SNR value as a function of the satellite elevation angle.
- Carry out link budget assessments, taking into account the possibility to modify values such as antenna characterization, satellite height, transmission power.
- Carry out performance assessments via link level simulations for both downlink and uplink transmissions. In particular, characterize the performance of the Narrow-

band Physical Downlink Shared Channel (NPDSCH) in terms of SNR or Spectral efficiency and BLER for each of the configurations, where different types of transmission will be modeled and different types of channel, AWGN and TDL will be analyzed. Parameters such as the number of repetitions, the number of subframes per transport block, IMCS, etc. will be modified. Furthermore, simulations will be carried out for different channel estimators. The results obtained will be measured in terms of SNR or Spectral efficiency for each of the configurations.

- Carry out performance assessments via link level simulations for both downlink and uplink transmissions. In particular, characterize the performance of the Narrowband Physical Uplink Shared Channel (NPUSCH) in terms of SNR or Spectral efficiency and BLER for each of the configurations. Configurations will be modified with different types of transmission, different numbers of tones or even modifying the channel model. Parameters such as the number of repetitions, the number of subframes per transport block, IMCS, etc. will be modified. Furthermore, simulations will be carried out for different channel estimators. The results will be presented in SNR values for a BLER of 10%, in addition to their corresponding spectral efficiency.

1.3 Structure of the document

The contents of this report are structured in four chapters:

Chapter 1 - Introduction:

This chapter provides a brief introduction to the context of the project, as well as the main objectives of the study.

Chapter 2 - NB-IoT protocol fundamentals:

This chapter provides a description of the NB-IoT protocol including features such as deployment modes, the grid resource, channels and signals used, as well as a section explaining the most relevant values to understand the subsequent simulations and a section explaining the adaptations of this protocol for NTN communications.

Chapter 3 - Characterization of a NB-IoT NTN deployment scenario:

This chapter provides a description of the scenario, such as the type of antenna, user's features or a description of the satellite, as well as the geometry associated with the scenario. In addition a satellite link budget study.

Characterization of the different scenarios with their corresponding equations, on the one hand the static study, where the footprint coverage of the satellite will be characterized, this case can be described for one beam or for multiple beam, pointing to Nadir or pointing to a specific direction. On the other hand the dynamic study is also studied, where the satellite pass is characterized, the Doppler effect and its variation over time, the variation of the SNR value as a function of the elevation angle and the propagation delay and how it varies over time.

Chapter 4 - Link level performance analysis:

This chapter provides a description of how it is modeling the transmission and reception as well as the channel, both AWGN and TDL and finally modeling of the Doppler effect.

Analyze the characteristics of the channel estimators.

Simulation results, both for the downlink communication study and for the uplink scenario. In both analyses, the effects or impacts produced by the type of channel estimator, the number of repetitions or the impact of the Doppler effect will be investigated.

2 NB-IoT NTN protocol fundamentals

2.1 Protocol basics

Narrowband IoT is a standard created by 3GPP standardization organization. It is the new narrowband radio technology developed for the Internet-of-Things (IoT). This standard was introduced in Release 13. With improvements that were reflected in the following releases, 14 and 15. Then in Release 15, NB-IoT was designed to enable 5G mMTC, and will continue to be relevant in the following releases, for example in Release 17 [12] where it is studied to support this technology in Non-Terrestrial Networks (NTN). In this first section, the fundamental aspects of NB-IoT will be discuss.

NB-IoT is a protocol that has been created to serve a high number of devices in the Internet of Things. NB-IoT uses the LTE architecture but removes a lot of complexity from the user and uses narrow-band transmissions to achieve a better link budget. NB-IoT is the technology that can provide service to the M-IoT communications and communications market. The most important features of NB-IoT that make this technology very promising for the future are the following[1]:

- Ability to connect more than 50000 users per channel, this is achieved due to the small amount of data transmitted by these devices and whose latency is not critical.
- Bandwidth of 180 kHz, which reduces costs when designing the transmitter, even in half-duplex operation avoids the need for a duplexer to separate the signals.
- Coexistence between 2G and 4G, due to the different operating modes: in band, guard band and standalone.
- The devices have an extended battery life, reducing power consumption by using eDRX (Externded discontinuous reception) or different operating modes that ensure energy conservation.
- Uses BPSK and QPSK modulation, this makes the devices cheaper and simpler to manufacture.

2.2 Deployment modes

NB-IoT systems require a bandwidth of 180 kHz to operate. This corresponds to a PRB in LTE technology. This is because NB-IoT can coexist with LTE technology, this coexistence allows to have 3 modes of operation:

- In-band: This case is when the NB-IoT radio subframe is located within the LTE bandwidth, occupying an LTE physical resource block (PRB) of the LTE band. In this case, the first 3 OFDM symbols are occupied by LTE control signals, so NB-IoT avoid these symbols.
- Guard-band: NB-IoT radio subframes are the guard bands that exist between LTE channels. As these bands would not be used by LTE, NB-IoT can use all the symbols of the subframe.

- Standalone: NB-IoT uses channels that are not being occupied by LTE spectrum, so it can occupy all the symbols in the subframe. Normally it can occupy a single GSM carrier of 200 kHz.

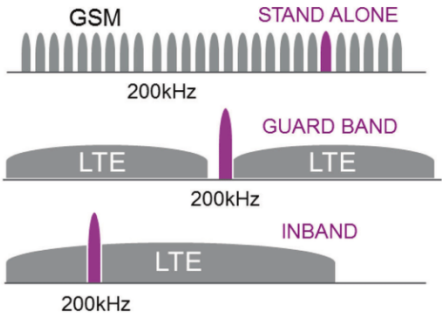

Figure 1: Deployment modes

Note that when the device operates in in-band mode, the NB-IoT signal can be positioned in different PRBs depending on the LTE bandwidth. The following table summarizes the locations.

LTE Bandwidth (MHz)	**PRB Positions for NB-IoT**
3	2,12
5	2, 7, 17, 22
10	4, 9, 14, 19, 30, 35, 40, 45
15	2, 7, 12, 17, 22, 27, 32, 42, 47, 52, 57, 62, 67, 72
20	4, 9, 14, 19, 24, 29, 34, 39, 44, 55, 60, 65, 70, 75, 80, 85, 90, 95

Table 1: Position intended for NB-IoT in the in-band mode

2.3 Resource grid

The NB-IoT downlink is based on OFDM symbols with 15 kHz carrier spacing and always using the 12 subcarriers. The resources are located as subframes, which span 1ms and contain 2 slots, each of 0.5ms with 7 OFDM symbols per slot. So, each subframe contains 2 PRBs. The downlink radio channel is estimated using Narrowband Reference Symbols (NRS), this signal occupies the last 2 OFDM symbols of each slot [1].

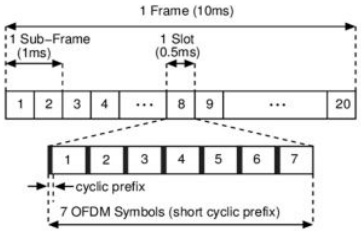

Figure 2: LTE physical frame, subframe, slot and symbol

In the uplink direction, Single-Carrier Frequency Division Multiple Access (SC-FDMA) would be used and the resources grid can be configured using a carrier spacing of 15 kHz or 3.75 kHz [19].

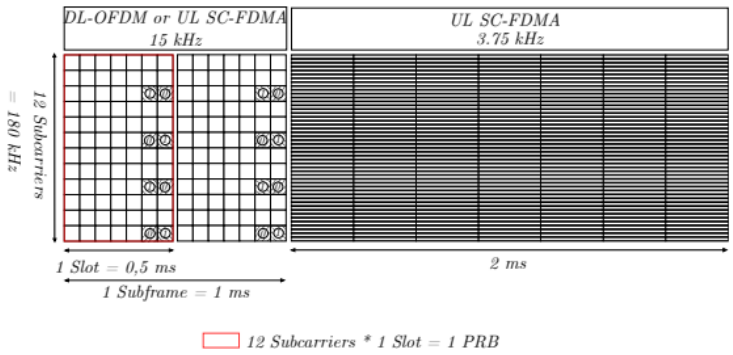

Figure 3: Resource grid

NB-IoT introduces the concept of Resource Units (RU) in uplink communications. This concept is based on being able to allocate one or more subcarriers of a single PRB for different users. These subcarriers are known as tones, so depending on the tones the configuration can be single or multi-tone operation.

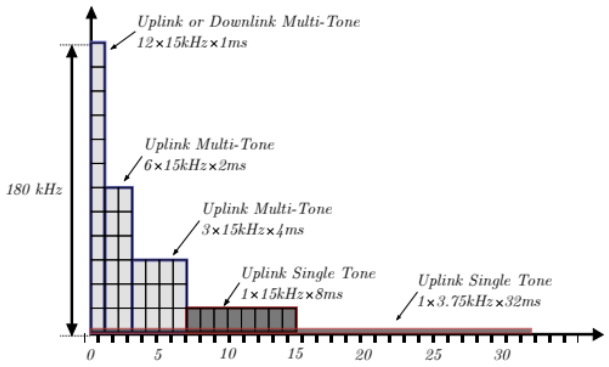

Figure 4: Different configuration of the subcarriers in the RU

In the case of DL communication, Orthogonal Frequency Division Multiple Access (OFDM) takes place. It multicarrier modulation extends the concept of single carrier modulation using 12 orthogonal subcarriers spaced 15 kHz, which is a resource block in LTE.

In DL the only modulation used is QPSK. Therefore, it only sends 2 bits per RE.

Regarding the UL scenario, Single-Carrier Frequency Division Multiple Access (SC-FDMA) is used, one of the main reasons for using this type of transmission technique is because the terminal has less capacity and is more limited in power, this technique makes the battery consumption is lower, and also the Peak-to-Average Power Ratio (PAPR) is lower compared to OFDM.

In UL, there are several transmission options depending on the number of tones used to transmit, as well as different subcarrier spacing (SCS) that can take value of 3.75kHz or 15 kHz as explained above.

Note that when using a SCS=3.75 kHz, the slot duration is 2 ms, which is 4 times longer than the duration of a slot with SCS=1 kHz, each RE has less BW. In the case of Multitones, the higher the number of all, the shorter the RU duration.

The modulation depends on the mode, in single-tone transmission the modulation can be $\frac{\pi}{2}$BPSK, $\frac{\pi}{4}$QPSK and in multitone transmissions, the modulation used is QPSK.

As a summary, the following table is presented:

Subcarrier Spacing	Number of Subcarriers	Number of Slots per RU	Number of RE per RU	Number of SC-FDMA Symbols	BW	Slot Duration [ms]	RU Duration [ms]
3.75	1	16	112	112	3.75	2	32
15 kHz	1	15	16	112	15	0.5	8
15 kHz	3	45	8	168	45	0.5	4
15 kHz	6	90	4	168	90	0.2	2
15 kHz	12	180	2	168	180	0.5	1

Table 2: Transmission configuration in UL

2.4 Channels and signals

The NB-IoT physical layer must fit the LTE physical layer although these physical channels and signals are adapted and modified to operate in the NB-IoT framework [1] [18].

Two parts can be distinguished, the downlink part and the uplink part.

In the downlink part, the following channels can be found.

- Narrowband Physical Broadcast Channel: This channel is responsible for transmitting information about the network configuration and cell information. MIBs (master information blocks) are transmitted on this channel. It has a periodicity of 64 frames and it is mapped in the subframe number 0 of each frame and occupies all the subcarriers.
- Narrowband Physical Downlink Shared Channel: This channel is dedicated to transmit user information and the control, acknowledgement (ACK) or negative acknowledgement (NACK) information of the Hybrid Automatic Repeat reQuest (HARQ) processes from the base station to the users. It could be assigned in all subframes except for 0, 5 and 9, which correspond to NPBCH, NPSS and NSSS respectively.
- Narrowband Physical Downlink Control Channel: On this channel all control signals concerning important processes such as paging, random access and data transmission are transmitted. It is assigned and allocated in the same form as the NPDSCH.

And the following signals could be found:

- Narrowband Primary and Secondary Synchronization Signals: These signals are transmitted in downlink to allow the devices to adjust the timing and frequency offsets of the UE. The NPSS signal allows to synchronize the device during initial acquisition without knowing the NB-IoT operation mode, this signal is sent in subframe number 5. The NSSS signal signals the cell ID, which is sent in subframe number 9.

  The allocation of resources within the NPSS and NSSS subframe is illustrated in the next figure.

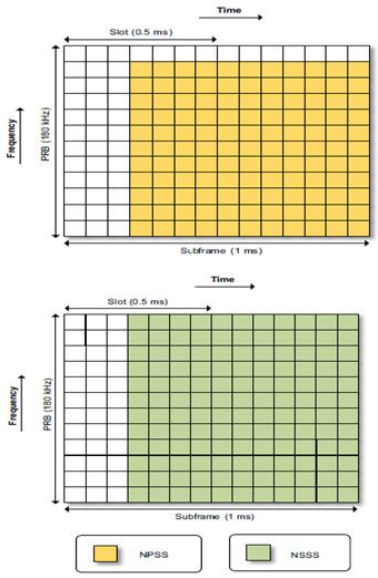

Figure 5: NPSS and NSSS allocation in the resource grid

- Narrowband Reference Signal: NRS is the signal that is used to allow the UE to perform downlink channel estimation. This signal can also be used for signal strength measurements and quality measurements. This signal is sent through port 0 (if there is only one antenna, if there are two it would be sent through port 0 and port 1). This signal is important for channel estimation, thanks to this estimation the system capacity is improved improving the system performance in terms of BLER.

  The assignment of resources for NRS inside the subframe is shown in the following figure.

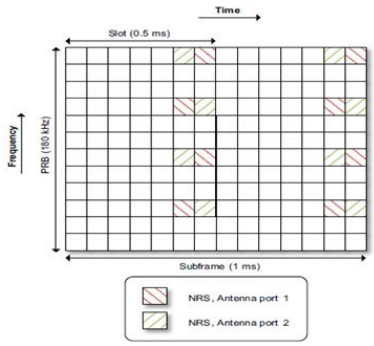

Figure 6: NRS allocation in the resource grid

An image is illustrated below with downlink physical channels.

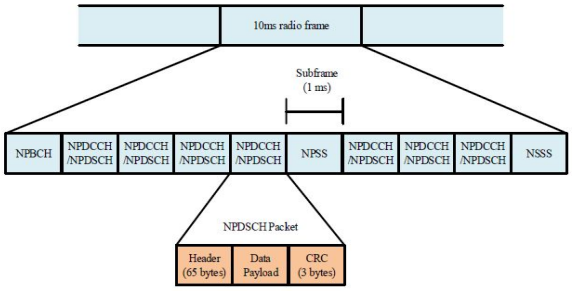

Figure 7: NB-IoT DL frame structure

In the uplink part, the following channels can be found.

- Narrowband Physical Random Access Channel: The NPRACH channel is used by the devices to access the network and synchronization for data transmission. This initial access establishes the radio link and scheduling request.
- Narrowband Physical Uplink Shared Channel: The NPUSCH channel is used to transmit user data from UEs to base stations or to send control information, ACK and NACK.

In UL, there is only one physical signal, it is the following:

- Demodulation reference signal: DMRS, also known as "uplink pilot", is used to estimate the channel in the frequency domain for uplink transmissions.

The assignment of resources for NRS inside the subframe is shown in the following figure.

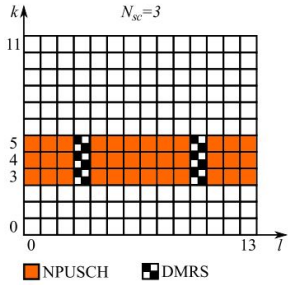

Figure 8: DMRS allocation in the resource grid

An image is illustrated below with uplink physical channels.

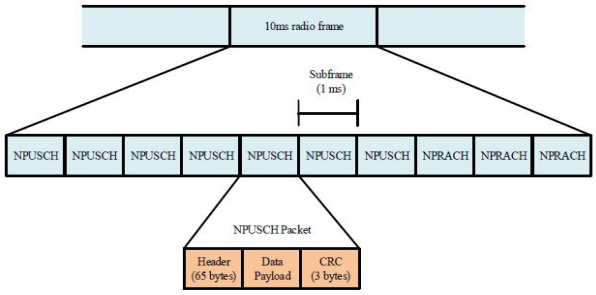

Figure 9: NB-IoT UL frame structure

2.5 Most relevant NB-IoT parameters for simulations

In order to explain the most important parameters that will be used in future simulations and to be more useful for the reader, this sub-section has been created. For this purpose it will be divided into two parts, one with reference to the NPDSCH and the other with reference to the NPUSCH.

2.5.1 NPDSCH parameters

All parameters that will be modified and used in the downlink simulations will be explained here.

- **ISF**

  The variable ISF configures the number of subframes for a NPDSCH according to 3GPP TS 36.213 Table 16.4.1.3-1. [14] Valid values for ISF are 0...7.

I_{SF}	N_{SF}
0	1
1	2
2	3
3	4
4	5
5	6
6	8
7	10

Table 3: Number of subframes for NPDSCH

- **Number of repetitions**

  The variable IRep configures the number of NPDSCH repetitions according to 3GPP TS 36.213 Table 16.4.1.3-2. [14] Valid values for IRep are 0...15.

I_{Rep}	N_{Rep}
0	1
1	2
2	4
3	8
4	16
5	32
6	64
7	128
8	192
9	256
10	384
11	512
12	768
13	1024
14	1536
15	2048

Table 4: Number of repetitons for NPDSCH

- **IMCS**

  The variable IMCS is the index which specifies which modulation and coding scheme would be used. Valid values for IMCS are 0...13.

- **TBS**

The variable transport block size (TBS) is configured according to 3GPP TS 36.213 Table 16.4.1.5.1-1 [14] using the values of the IMCS variable together with the IRep.

I_{TBS}	I_{SF}							
	0	1	2	3	4	5	6	7
0	16	32	56	88	120	152	208	256
1	24	56	88	144	176	208	256	344
2	32	72	144	176	208	256	328	424
3	40	104	176	208	256	328	440	568
4	56	120	208	256	328	408	552	680
5	72	144	224	328	424	504	680	872
6	88	176	256	392	504	600	808	1032
7	104	224	328	472	584	680	968	1224
8	120	256	392	536	680	808	1096	1352
9	136	296	456	616	776	936	1256	1544
10	144	328	504	680	872	1032	1384	1736
11	176	376	584	776	1000	1192	1608	2024
12	208	440	680	904	1128	1352	1800	2280
13	224	488	744	1032	1256	1544	2024	2536

Figure 10: Transport Block size table for NPDSCH

2.5.2 NPUSCH parameters

All parameters that will be modified and used in the uplink simulations will be explained here.

- **Number of RU**

  Resource units (RU) are used to describe the mapping of the NPUSCH to resource elements. A RU is defined as N_{symb}^{UL} and N_{slots}^{UL} consecutive SC-FDMA symbols In the time domain and N_{sc}^{RU} consecutive subcarriers in the frecuency domain, where N_{sc}^{RU} and N_{symb}^{UL} are given in the table 10.1.2.3-1 [15].

NPUSCH format	Δf	N_{sc}^{RU}	N_{slots}^{UL}	N_{symb}^{UL}
1	3.75 kHz	1	16	7
	15 kHz	1	16	
		3	8	
		6	4	
		12	2	
2	3.75 kHz	1	4	
	15 kHz	1	4	

Figure 11: Supported combinations of N_{symb}^{UL}, N_{sc}^{RU} and N_{slots}^{UL}

The number of subcarriers used for NPUSCH, N_{sc}^{RU}, depends on the NPUSCH format and subcarrier spacing as shown in the table. There are 1,3,6 or 12 continuous subcarriers for NPUSCH

The number of RU is computed with table 16.5.1.1-2 [15].

I_{RU}	N_{RU}
0	1
1	2
2	3
3	4
4	5
5	6
6	8
7	10

Table 5: Number of resource units for NPUSCH

- **Number of repetitions**

  The variable IRep configures the number of NPUSCH repetitions according to 3GPP TS 36.213 Table 16.5.1.1-3. [14] Valid values for IRep are 0...7.

I_{Rep}	N_{Rep}
0	1
1	2
2	4
3	8
4	16
5	32
6	64
7	128

Table 6: Number of repetitions for NPUSCH

- **NPUSCH format and TBS**

  There are two payload types defined for NPUSCH transmission, format 1 (”Data”) and format 2 (”Control”). For format 1, the UE uses the combination of the modulation and coding scheme (MCS) and the resource allocation signaled through the DCI to determine the transport block size (TBS) of the set defined in TS 36.213 Table 16.5.1.1.2-2 [14].

I_{TBS}	I_{RU}							
	0	1	2	3	4	5	6	7
0	16	32	56	88	120	152	208	256
1	24	56	88	144	176	208	256	344
2	32	72	144	176	208	256	328	424
3	40	104	176	208	256	328	440	568
4	56	120	208	256	328	408	552	680
5	72	144	224	328	424	504	680	872
6	88	176	256	392	504	600	808	1000
7	104	224	328	472	584	712	1000	1224
8	120	256	392	536	680	808	1096	1384
9	136	296	456	616	776	936	1256	1544
10	144	328	504	680	872	1000	1384	1736
11	176	376	584	776	1000	1192	1608	2024
12	208	440	680	1000	1128	1352	1800	2280
13	224	488	744	1128	1256	1544	2024	2536

Figure 12: Transport Block size table for NPUSCH

For format 2, the NPUSCH carries the 1-bit ACK/NACK.

In this study, only format 1, in which useful data is sent, will be considered.

2.6 Adaptations for NTN

Non-terrestrial networks (NTNs) are a potential solution to complement terrestrial networks to obtain global coverage. This NTN uses radio frequency resources that would be placed on a satellite. The main function of NTNs is to complement the services of a cellular network, in places where the terrestrial network cannot provide service. Therefore, NTN networks are very likely to be used in combination with the NB-IoT protocol to provide global coverage of IoT devices.

In order to adapt NB-IoT in satellite systems, the NB-IoT protocol needs to be modified, an important part of it is the physical layer. The major challenge is to be able to deal with random access (RA). This process is in charge of scheduling data transmission and synchronization of devices. This process cannot support the satellite channel improvements, these would be two main ones, the first one is the long propagation delays, these delays depend on the satellite orbit and elevation angle. The other aspect is the large Doppler effect, due to the high speed of movement of LEO satellites, a high Doppler shift is introduced in the NB-IoT signal, this aspect can be balanced with a compensation technique, but there would be a residual Doppler that will be studied later.

The NB-IoT NTN protocol will be expected to operate with constellations of LEO satellites. Based on the NB-IoT protocol that was created for terrestrial access, the features of communication between LEO satellites, such as satellite channel characteristics, as well as improvements to deal with a long propagation delay, and new mechanisms to compensate for the Doppler effect, have been incorporated into the NB-IoT protocol.

Regarding the future Release 17 specifications, the following are included [2]:

- NR NTN Protocols: Enhanced New Radio (NR) protocol for NTN, intended for satellite mobile broadband services.

- IoT NTN protocols: enhanced Cellular IoT (CIoT) protocols (i.e. NB-IoT and eMTC) for NTN, intended for mMTC services from satellite platforms.

In addition the NTN adaptations for NB-IoT will try to support different scenarios, such as GEO and NGSO constellations.

These adaptations are as follows:

- Mechanisms for Uplink pre-compensation at the UE side of time and Doppler frequency shifts and DL frequency synchronisation enhancements.
- Timing relationships adjustments and new time offsets in the different protocol procedures (random access, contention resolution, scheduling, hybrid automatic repeat request, etc.) to compensate for satellite propagation delays.
- System information enhancements, with the broadcasting of satellite ephemeris information.
- Mobility management improvements to cope with moving satellite cells and enhancements to tracking area management using the earth-fixed Tracking Area (TA) concept.
- Support of discontinuous coverage of the service link, without excessive UE power consumption and without excessive failures / recovery actions.

This whole study is developed assuming two important things, the UE has GNSS capabilities and the satellites' payloads are transparent, so that the network processing capabilities are on the ground are on the ground and the satellite is strictly used as a repeater.

3 Characterization of a NB-IoT NTN deployment scenario

3.1 Scenario description

The scenario considered in the study is based on a generic NB-IoT deployment using nanosatellites in LEO constellations.

In this chapter the NB-IoT NTN scenario is characterized based on some inputs on which to build the characterization. These basic elements are:

- NTN parameters, such as the spherical geometry of the Earth, the satellite's orbit or parameters associated with the satellite's motion, for example the satellite's speed.
- Satellite height, in this case a LEO satellite. However, any type of satellite is possible to characterize.
- Link budget parameters. The main parameters to be considered are transmitted power, frequency and gain of the antenna.
- Antenna information, for both IoT device and satellite. The program has been created in such a way that different antenna options can be incorporated:
  - Antenna type and the parameters that characterize this antenna.
  - From the radiation pattern, either from the θ/φ model or elevation/azimuth model.

  The pointing direction of the antenna can be configured by indicating the pointing angles in terms of θ or φ or even in terms of azimuth, az and elevation, el.

All these inputs make it possible to characterize the following outputs:

- Characterization of the satellite coverage footprint.
  - DL and UL SNR heatmap representation
  - DL and UL SNR statistics and CDF
- Characterization of the radiation pattern for any angle.
- Characterization over the satellite pass.
  - DL and UL SNR time evolution over a satellite pass
  - "Doppler shift" (Hz) and "Doppler shift variation" (Hz/s)e volution over a satellite pass.
  - "Delay" (ms) and "Delay variation" (ms/s) evolution over a satellite pass

3.1.1 Antenna characterization

The program that has been created for this study allows to use any antenna that can be created with the MATLAB Antenna Toolbox. It is possible to simulate many types

of antennas, such as a dipole, monopole, helix antenna, microstrip, as well as to create arrays of antennas. It is also possible to create antennas from electric fields.

In addition, these antennas or antenna arrays have the possibility of orienting their point to Nadir at certain angles, as will be seen in the following sections.

In this study, all the analysis has been carried out according to the spherical coordinates using the angles θ and φ, as shown in the following image.

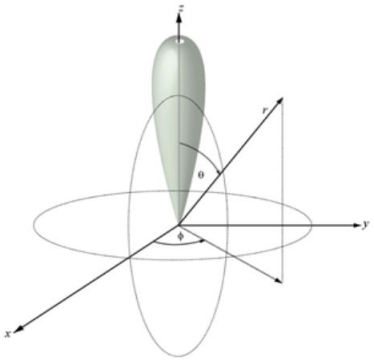

Figure 13: Reference spherical coordinate axes

The antenna is incorporated into the program by means of its radiation pattern. It is possible to incorporate it based on el and az angles or θ and φ angles.

This provides the freedom to characterize the scenario for any type of antenna.

In this study, all simulations have been performed with a 2-element linear array (circular microstrip patch).

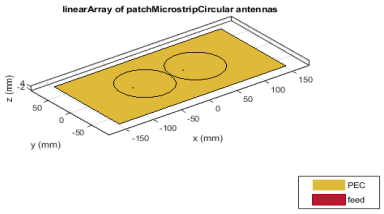

Figure 14: Antenna 2-element linear array

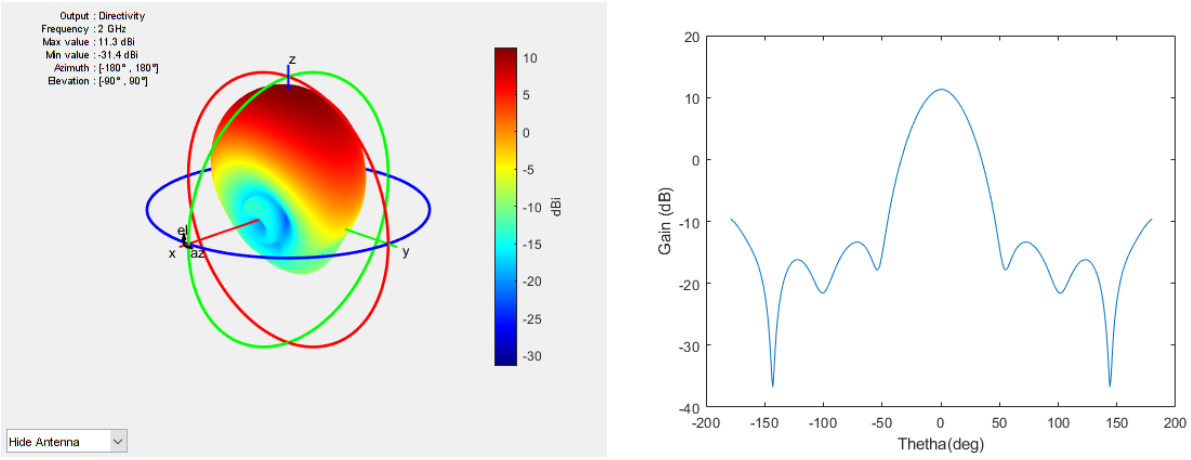

(a) (b)

Figure 15: Antenna pattern from MATLAB Toolbox (a) and 2-D radiation pattern (b)

The radiation pattern of this antenna is expressed in azimuth, az and elevation angles, el.

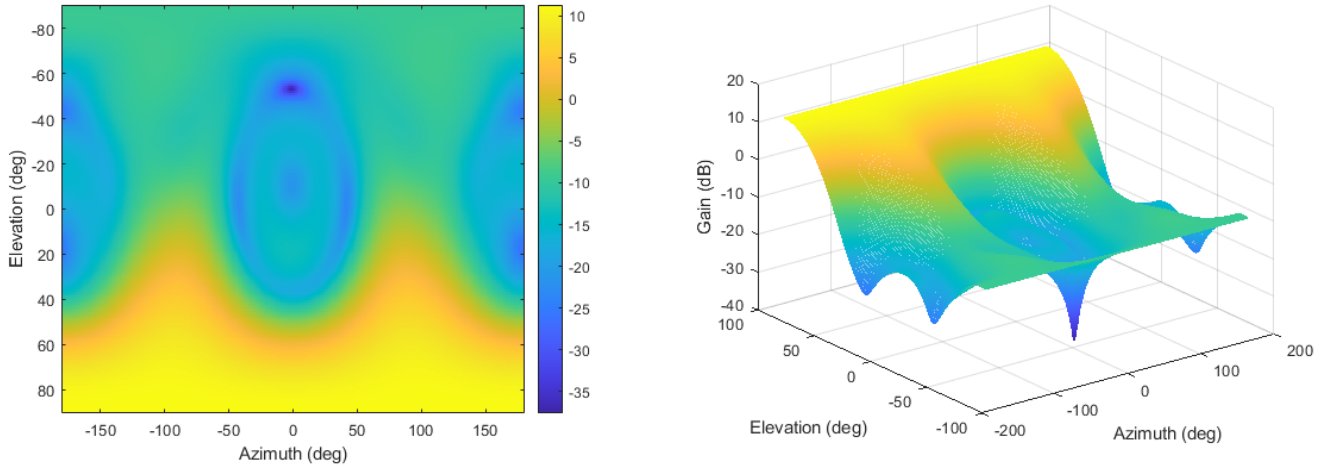

(a) (b)

Figure 16: Radiation pattern in terms of az and el

The radiation pattern can be used to characterize the antenna gain as a function of theta, θ and phi, φ angles, angle conversion has been performed, the final radiation pattern is shown in the following image.

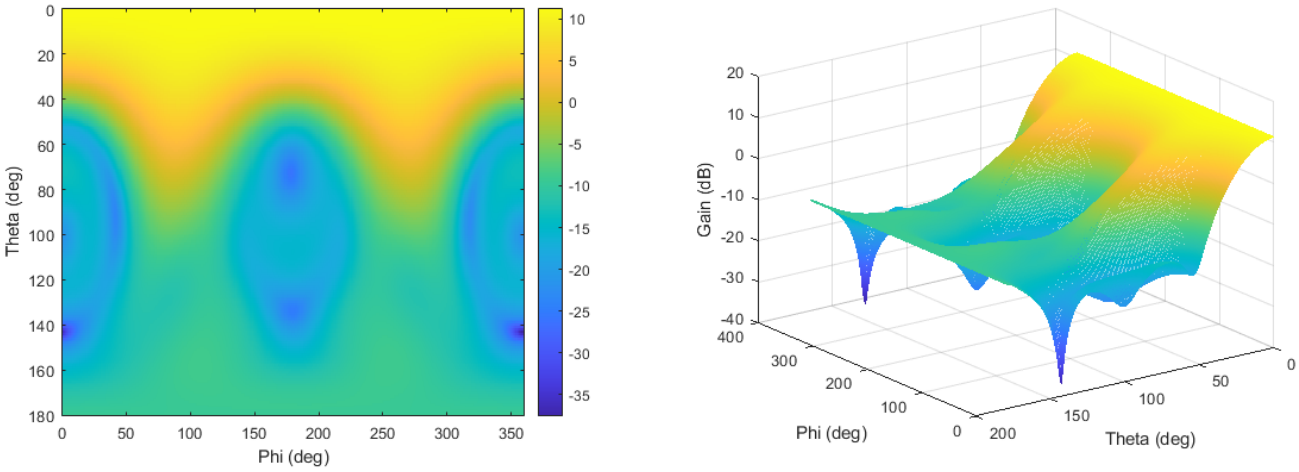

(a) (b)

Figure 17: Radiation pattern in terms of θ and φ

Another interesting aspect to review is the directivity of the antenna, this value is 11.3 dB. In addition, graphs of an important parameter are obtained which is the Half Power Beam Width (HPBW), this is divided in two, one corresponds to the orthogonal direction of the satellite movement and is known as Horizontal HPBW (H-HPBW) and the other is the HPBW in the direction of the satellite orbital movement, referred to as Vertical HPBW (V-HPBW).

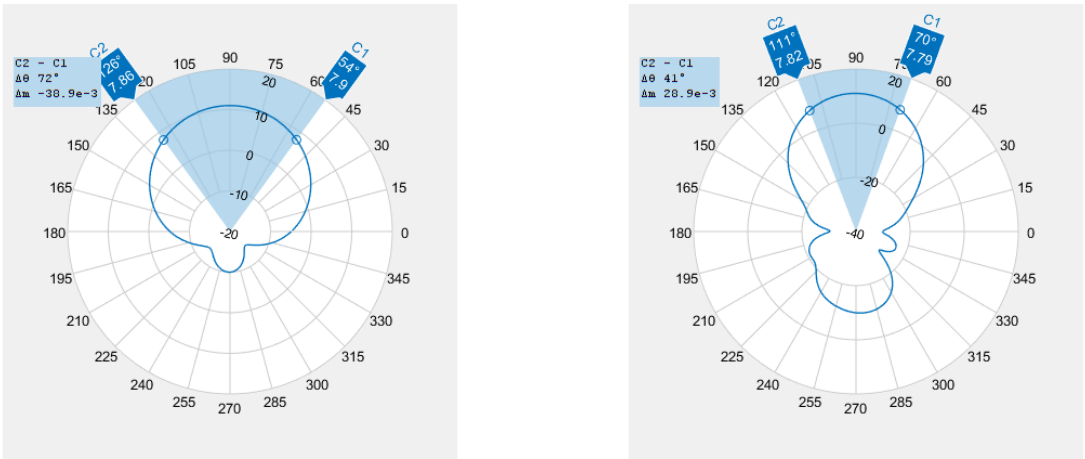

(a) (b)

Figure 18: Horizontal HPBW (a) and Vertical HPBW (b)

Looking at the polar shape, it can be seen that the H-HPBW is larger and the V-HPBW is narrower. This configuration allows for a wider satellite swath while reducing the duration

of the access time.

3.1.2 User

The user to be characterized in this scenario is the standard IoT device transmitting at a power of 200mW (equivalent to 23 dBm) [3].

It is assumed that this NB-IoT device contains a GNSS module to know its location. In addition the satellite transmits via broadcast the position and velocity information of the satellite, using this data the user is able to compensate for the doppler effect.

If the UE knows its own position and the velocity and position of the satellite, it can calculate and compensate for the Doppler effect and propagation delays.

3.1.3 Satellite

All the parameters that have been used and taken into account related to the satellite, such as dimensions, satellite orbit or transmitted power, are explained in this section.

3.1.3.1 Satellite parameters

In this study, a CubeSat has been considered, the use of nanosatellites for delivery of IoT, is growing in popularity due to its low fabrication costs and its great utility in the creation of nano-satellite constellations. The space of a CubeSat is measured in U, each U is a cube of 100 x 100 x 100 [mm]. This means that the space available to place the solar panels, which supply energy to the satellite, and the antennas, is reduced, as well as reducing the RF systems.

As there are many considerations when building a nanosatellite, such as size or power limitations, one aspect to emphasize is the antenna, since it has very limited volume to be able to assemble them, in addition to a very small surface that would point to Nadir(towards the Earth). In addition, it must be taken into account that external elements cannot be added, since there are deployer limitations [2].

Therefore, in this study, the satellite antenna can be modified as seen in the previous section, both for the satellite and the NB-IoT user. The most usual case in the satellite is to use a microstrip patch antenna designed to operate in the 2 GHz band. So, it has been decided to use this type of antenna

The transmit power of the satellite would be about 2W (equivalent to 33 dBm) for a CubeSat of about 1U [3].

3.1.3.2 Orbit and speed parameters

To characterize the orbit parameters [3], it has been considered that the earth is a sphere with a radius $R_E = 6357[km]$. The satellite orbits the earth in a Kepler orbit at an altitude of $h_s = 550[km]$ with respect to the surface of the earth. The velocity of the satellite can be calculated from the following formula: $v_{sat} \approx \sqrt{(G \cdot M_e/(R_E + h_s))}$, The velocity of the satellite is obtained as $v_{sat} = 7.57[km/s]$. Where the mass of the earth is considered as $M_e = 5.972 \cdot 10^{24}[kg]$ and the rotational speed of the earth as $V_e = 460[m/s]$.

3.1.4 Scenario geometry

The geometry of the satellite-device link is represented as follows:

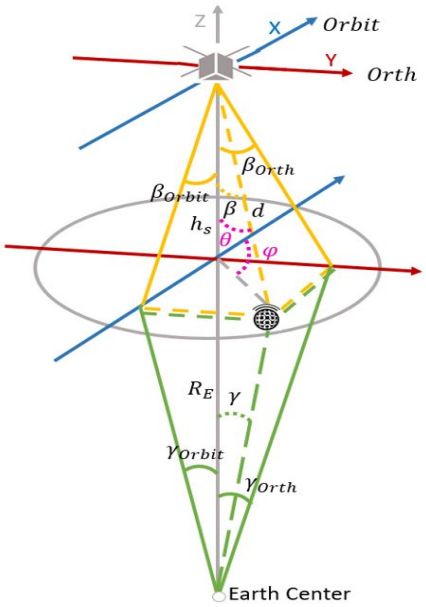

Figure 19: Scenario geometry

The figure shows the main parameters that characterize the scenario. The earth curvature is taken into account in the model although it is not shown in the figure.

The angle β, is the angle between the UE and the nadir direction as observed from the satellite. This angle can be given in the orbital plane, denoted as β_{orbit}, or in the orthogonal plane, denoted by $\beta_{orthogonal}$.

Another important angle is γ, it is the angle formed by the UE with the nadir direction as observed from the Earth center, this angle is important since it does not depend on the height of the satellite. Like the previous angle, γ can be given in the orbital plane, denoted as γ_{orbit} or in the orthogonal plane, denoted as $\gamma_{orthogonal}$.

The distance between the UE and the satellite is denoted by d.

The angles θ and φ, which would correspond to the spherical coordinates of the point with respect to the satellite antenna, can also be observed. The maximum of the satellite antenna is oriented in the nadir direction of the satellite.

3.2 Satellite link budget formula

In a telecommunication system, a useful analysis is the link budget. A link budget is an accounting of all the power gains and losses that a communication signal suffers in a telecommunication system. This signal is sent from a transmitter through a communication medium to the receiver. It is an equation that provides the received power from the

transmitter power, after attenuation of the transmitted signal due to propagation losses of the medium, as well as antenna and feedline gains and other losses, and amplification of the signal at the receiver [3] [4].

Using the link budget, it is possible to calculate how much power of the transmitted signal finally reaches the receiver. This is used to ensure that the information arriving at the receiver is correctly intelligible and correctly understood.

By neglecting the interference, the formula used is as follows:

$$SNR_{DL} = P_{tx_{Sat}} - P_{Noise} - P_{athloss} + G_{UE_{Ant}} + G_{SAT_{Ant}} + G_{Shadow} + G_{PolarMiss} + G_{absorption} + G_{scintillation} \quad (1)$$

Let us now clarify all the parameters one by one.

- $P_{tx_{Sat}}$ and $G_{SAT_{Ant}}$:The first parameter corresponds to the transmitted power at the transmitter, in this case as it is a DL communication, it would be the power transmitted by the satellite, the second parameter corresponds to the gain of the transmitting antenna, in this case it corresponds to the gain of the satellite antenna. Both variables combined create the EIRP, which is the effective isotopic radiated power. It can be calculated as:

$$EIRP = P_{tx_{Sat}} + G_{SAT_{Ant}} \quad (2)$$

- P_{Noise}: This parameter is the noise power, this noise power is calculated as the thermal noise at the receiver with the following equation:

$$P_{Noise} = 10 \cdot \log_{10}(K \cdot B_{DL} \cdot (T_{a_{UE}} + T_0 \cdot (10^{\frac{NF_{UE}}{10}} - 1))) + 30(dBm) \quad (3)$$

  where NF_{UE} represents the UE noise figure, T_a represents the antenna temperature, T_0 represent the ambient temperature, B_{DL} is the bandwidth and K is the Boltzmann constant.

- $P_{athloss}$ This parameters represents the free space path loss and the equation is the following:

$$P_{athloss} = 10 \cdot \log_{10}((\frac{4 \cdot \pi \cdot d}{\frac{c}{f}})^2) \quad (4)$$

  Where c is the speed of light, f is the carrier frequency and d is the slant range, It should be noted that propagation losses will be computed according to the free space model. The slant range is calculated as follows:

$$d = \sqrt{(h_s + R_E)^2 + R_E^2 - 2 \cdot R_E \cdot (R_E + h_s) \cdot \cos\gamma} \quad (5)$$

  This equation represents the distance from the satellite to the UE. This equation depends on the radius of the earth R_E, the height of the satellite h_s and γ It is the angle of elevation between the center of the earth and the UE.

- $G_{UE_{Ant}}$ is the gain of the UE antenna, it is assume that this parameter is equals to 0.

- G_{Shadow}, $G_{PolarMiss}$, $G_{absorption}$ and $G_{scintillation}$: G_{Shadow} is the loss caused by shadowing, $G_{PolarMiss}$ is the loss caused by the polarization mismatch, $G_{absorption}$ is the loss caused by the atmospheric absorption and finally $G_{scintillation}$ correspond to the loss due to scintillation.

For UL, the equation will be as follows:

$$SNR_{UL} = P_{tx_{UE}} - P_{Noise} - P_{athloss} + G_{UE_{Ant}} + G_{SAT_{Ant}} + G_{Shadow} + G_{PolarMiss} + G_{absorption} + G_{scintillation} \quad (6)$$

The only change would be in the noise power which would now be characterized with the equation:

$$P_{Noise} = 10 \cdot \log_{10}(K \cdot B_{UL} \cdot (T_{a_{Sat}} + T_0 \cdot (10^{\frac{NF_{Sat}}{10}} - 1))) + 30(dBm) \quad (7)$$

The values used for these variables are shown in the following table:

Parameters	Downlink	Uplink
Carrier frequency (GHz)	2	2
Bandwidth (kHz)	180	3.75, 15, 45, 90, 180
Satellite height (km)	600	600
Boltzmann constant	$1.38064852 \cdot 10^{-23}$	$1.38064852 \cdot 10^{-23}$
Ambient Temperature (K)	290	290
Antenna Temperature (K)	290	290
Transmitted power (dBm)	33	23
Noise Figure (dBm)	7	5
Antenna Gain (dB)	$t(\theta, \varphi)$	0
Shadow Losses (dB)	-3	-3
Polar Mismatch losses (dB)	-3	-3
Absorption losses(dB)	-0.1	-0.1
Scintillation losses(dB)	-2.2	-2.2

Table 7: Link parameters

Note that the antenna gain depends on the radiation pattern of the antenna and the point where the user is located, expressed in the angles θ and φ.

3.3 Scenario characterization

In this section the geometry of the scenario described in section 3.1.4 will be studied in more detail, studying all the formulas and the most important parameters to be taken into account for the further study. This model will be divided in two parts, the first one will correspond to the static study, where only a snapshot of the satellite trajectory over the beam will be taken into account, in the second part a dynamic model will be studied, where studies of how the Doppler shift or the propagation delay varies according to the satellite path will be carried out.

3.3.1 Model with equations

To start the calculations, the starting point is a point X located on the surface of the Earth. This point can be described with the coordinates γ_{orbit} and γ_{orth}. This scenario could also be started from the same point X but described with the coordinates β_{orbit} and β_{orth} but for this case would depend on the value of the height of the satellite, using the first approach, would calculate the value of γ without needing to know the height of the satellite.

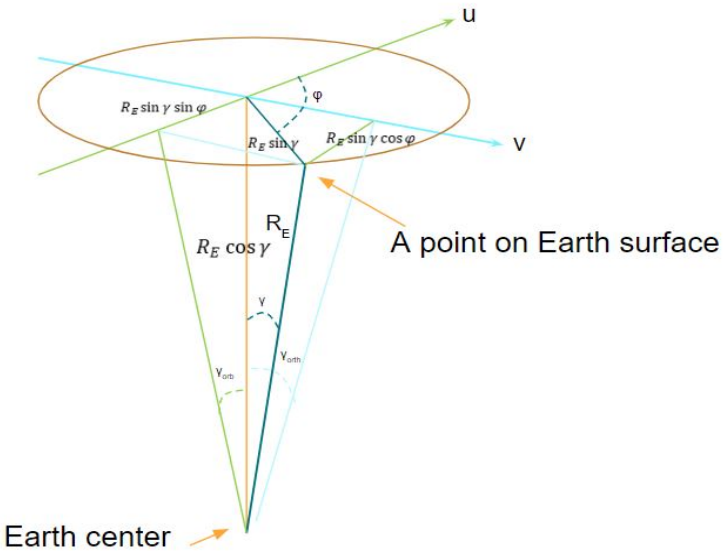

Figure 20: Coordinates transformations: focus is on angles as seen from Earth center

Once the starting point is defined, and the values of the γ_{orbit} and γ_{orth} coordinates are known, the values of γ and φ can be calculated using geometric formulas. The equations would be as follows:

$$\varphi = \tan^{-1}\left(\frac{\tan(\gamma_{orth})}{\tan(\gamma_{orbit})}\right) \tag{8}$$

$$\gamma = \tan^{-1}\sqrt{(\tan(\gamma_{orbit}))^2 + (\tan(\gamma_{orth}))^2} \tag{9}$$

Proof:

$\tan(\gamma_{orbit}) = \frac{R_E \cdot \sin(\gamma) \cdot \cos(\varphi)}{R_E \cdot \cos(\gamma)} = \tan(\gamma) \cdot \cos(\varphi)$

$\tan(\gamma_{orth}) = \frac{R_E \cdot \sin(\gamma) \cdot (\varphi)}{R_E \cdot \cos(\gamma)} = \tan(\gamma) \cdot \sin(\varphi)$

$\frac{\tan(\gamma_{orbit})}{\tan(\gamma_{orth})} = \tan(\varphi)$

$\tan(\gamma_{orbit})^2 + \tan(\gamma_{orth})^2 = \tan(\gamma)^2 \cdot \cos(\varphi)^2 + \tan(\gamma)^2 \cdot \sin(\varphi)^2 = \tan(\gamma)^2 \cdot (\cos(\varphi)^2 + \sin(\varphi)^2) = \tan(\gamma)^2$

After these parameters are calculated, the angle θ, the distance d, and the terminal elevation angle (α) can be further calculated.

To calculate the value of d the cosine theorem will be used obtaining the following equation:

$$d = \sqrt{(h_s + R_E)^2 + R_E^2 - 2_E(R_e + h_s) \cdot \cos(\gamma)} \tag{10}$$

Now d can be related to γ by the following formula.

$$\sin(\theta) \cdot d = R_E \cdot \sin(\gamma) \tag{11}$$

By subtracting θ let's obtain:

$$\theta = \sin^{-1} \frac{R_E \cdot \sin(\gamma)}{d} \tag{12}$$

Finally, it would remain to calculate the elevation angle of the terminal, this angle is the angle formed by the terminal pointing to the satellite with the horizon, as can be seen in the image:

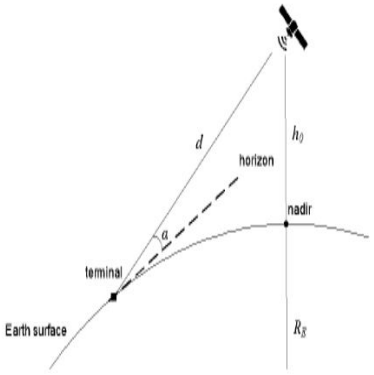

Figure 21: Illustration of elevation angle

If defining a triangle as follows:

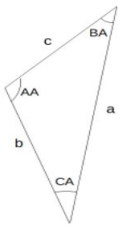

Figure 22: Illustration of a triangle

It can be clearly deduced that :

$$AA = 90 + \alpha \tag{13}$$

So

$$90 + \alpha + \gamma + \theta = 180 \tag{14}$$

By subtracting the final equation is obtained:

$$\alpha = 90 - \gamma - \theta \tag{15}$$

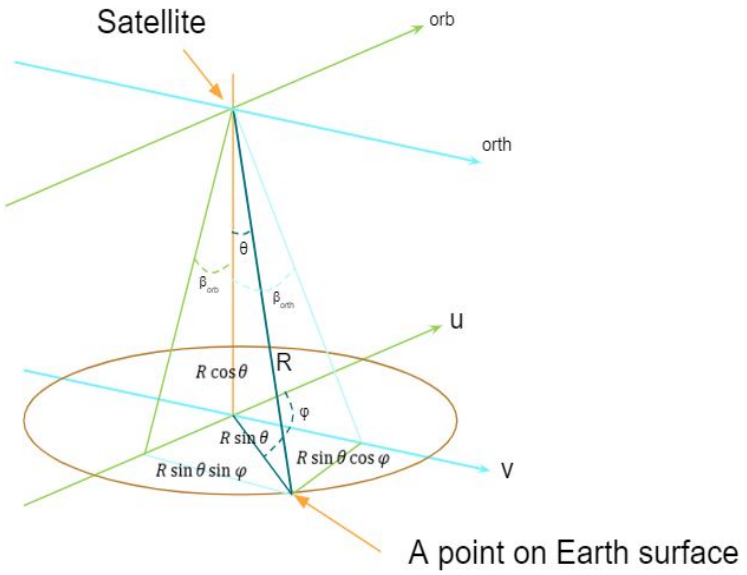

Figure 23: Coordinates transformations: focus is on angles as seen from satellite

With this the scenario would be described, it is also possible to use geometric formulas to calculate the values of β_{orbit} and β_{orth} in case they are needed. These two values would be modeled with the following equations:

$$\beta_{orbit} = \tan^{-1}(\tan(\theta) \cdot \cos(\varphi)) \tag{16}$$

$$\beta_{orth} = \tan^{-1}(\tan(\theta) \cdot \sin(\varphi)) \tag{17}$$

The proof is similar to the one explained above for the values of φ and γ so no formulas will be derived.

Using these formulas, the parameters used in the SNR calculations can be obtained.

3.3.1.1 Static study

In this first section the static scenario will be studied, in other words, where only a snapshot of the satellite is considered, this case will be studied in different ways. It will be possible to characterize the satellite coverage, as well as to analyze the different statistics in terms of SNR. In addition, it will be possible to observe and characterize different cases, where the satellite has one or several antennas, which creates one or several beams on the surface of the Earth and at the same time, it has been characterized that the tilt of the antenna can be pointing to Nadir or to some defined angles.

3.3.1.1.1 Characterization of the satellite coverage footprint (UL and DL SNR heatmap representation)

A useful way to visualize the coverage of the satellite, would be to see what are the dimensions of the foodprint that generates on the surface of the earth, if this is added to the option to see what is the SNR at each point, it could give a great idea of the surface that could cover for a certain range of SNR.

In this study a heatmap has been made to visualize the SNR value at each point of the surface. This foodprint is described as a function of the angles γ_{orbit} and γ_{orth}. These angles can be described in radians or degrees, but in order to get a more concrete and more feasible idea, it has been decided to express them in km, which is usually more usual.

In order to obtain the conversion of angles to kilometers, the curvature of the earth has been taken into account, the length is shown as the red line in the following figure:

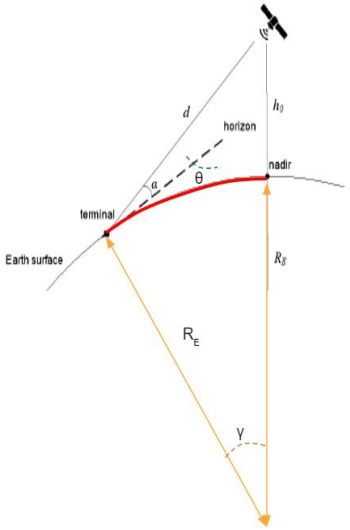

Figure 24: Characterization of the longitude in the scenario

And the formula relating that would be as below:

$$L = R_E \cdot \gamma(rad) \tag{18}$$

Taking into account these aspects, together with the values obtained from the link budget for the SNR calculation and taking into account that the antenna used is a Linear array 2 elements (circular microstrip patch), the following results can be visualized.

A contour line system has also been created within the heatmap, to see the curves of the different SNRs and also to be able to calculate the area of each SNR. This would be useful to be able to analyze the coverage area for an SNR greater than a certain value.

The area results can be measured as $Area(SNR \geq X(dB))$.

An example of how the heatmap would be represented would look like this:

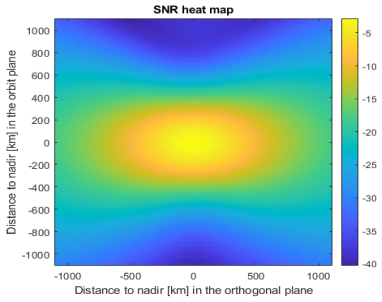

Figure 25: SNR heatmap

3.3.1.1.2 UL and DL SNR statistics and CDF

Another convenient way to analyze the results obtained in this characterization of satellite communication is by means of statistics. In this case, the statistics of the SNR parameter will be studied.

For this purpose, the following values have been calculated:

- Total number of samples
- Mean, it is the average value of the data set.
- Minimum value
- Maximum value
- Range, is a measure of dispersion, it indicates the difference between the maximum and minimum value of the data set.
- Median, measures the middle number of a group of values.
- Mode, measures the most repeated value within the data set.
- Variance, is a measure of dispersion, represents the variability of the data with respect to its mean.
- Standard deviation, measures the average dispersion of the variable, it indicates whether the values are more or less close to the mean. The deviation is the positive square root of the variance.

It is also possible to perform this statistical study in a more graphical representation. For this purpose, a histogram will also be made, in which it is possible to see how often the different SNR values are obtained and to see their distribution. In addition, the cumulative distribution function (CDF) will be calculated and shown graphically. This function specifies the probability that a random variable is less than or equal to a given value. In this case the random variable is the SNR.

All these values will be collected and grouped in the following cases, separately if the scenario is DL or UL.

Note that SNR values below 20 dB have been omitted for this analysis.

3.3.1.1.3 One beam

This section corresponds to the characterization in which the satellite has only one radio frequency system, so it will only have one beam. Two cases are going to be seen in this section, the antenna points to the Nadir direction, or the antenna is oriented to specific angles.

3.3.1.1.4 Antenna direction to nadir

This scenario is the most straightforward, the satellite antenna points to Nadir.The antenna as mentioned above is a Linear array 2 elements (circular microstrip patch)

The scenario could be represented as follows:

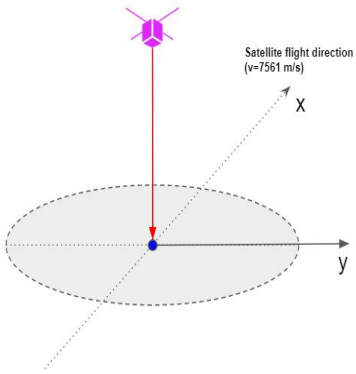

Figure 26: Characterization of the scenario where the antenna orientation is Nadir

The gain of the antenna would be oriented to Nadir, and expressed in the angles γ_{orbit} and $\gamma_{orthogonal}$ as shown in the following image:

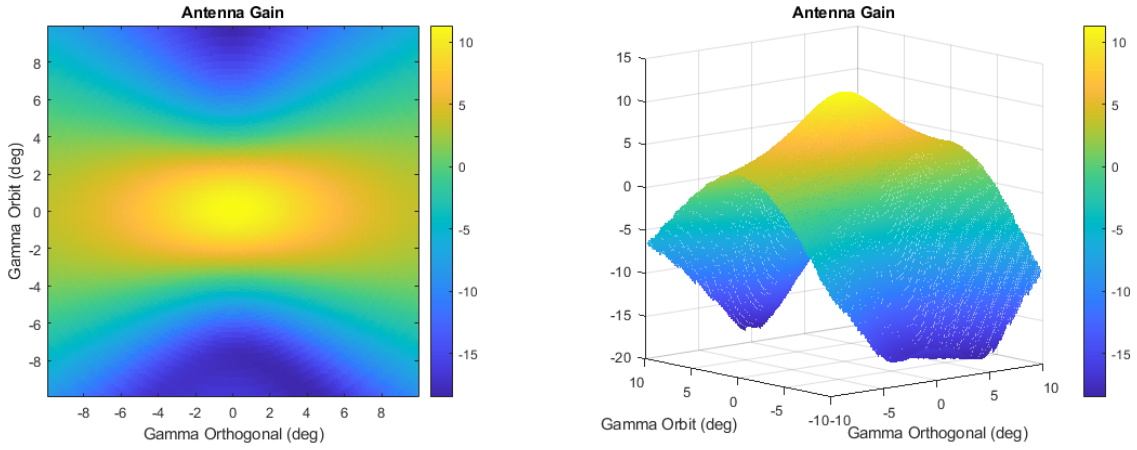

(a) (b)

Figure 27: Radiation pattern (a) and 3-D radiation pattern (b) in the scenario with Nadir orientation

In the first instance, the characterization has been performed for the downlink case. Therefore, an SNR heatmap is obtained such that:

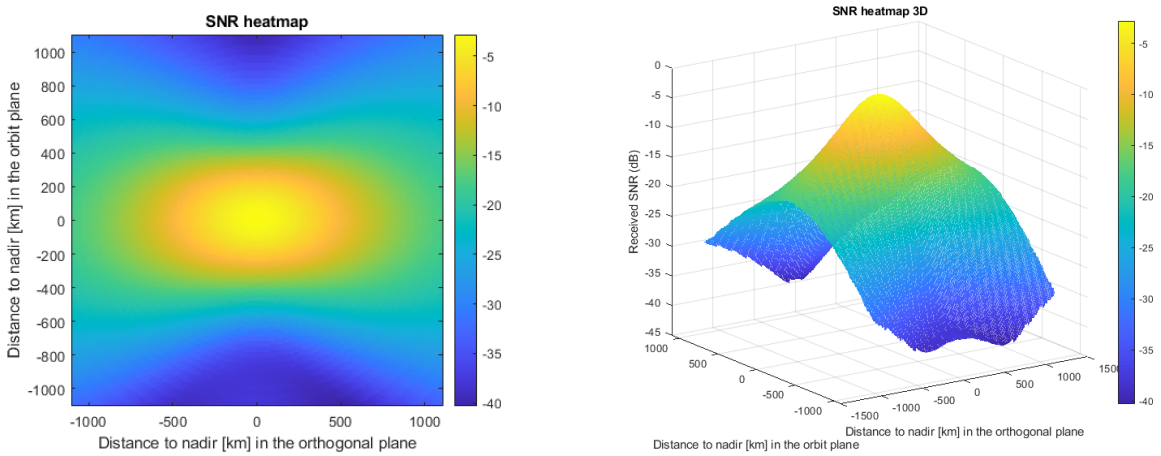

(a) (b)

Figure 28: SNR heatmap (a) and 3-D SNR heatmap (b) in DL scenario with Nadir orientation

With the following statistics:

Statistical parameter	Value
Total number of samples	17253
Mean	-13.686
Minimum value (dB)	-19.997
Maximum value (dB)	-2.815
Range	17.1847
Median	-14.7516
Mode	-2.8256
Variance	20.414
Standard deviation	4.5182

Table 8: Statistical values SNR DL for one beam in the Nadir direction

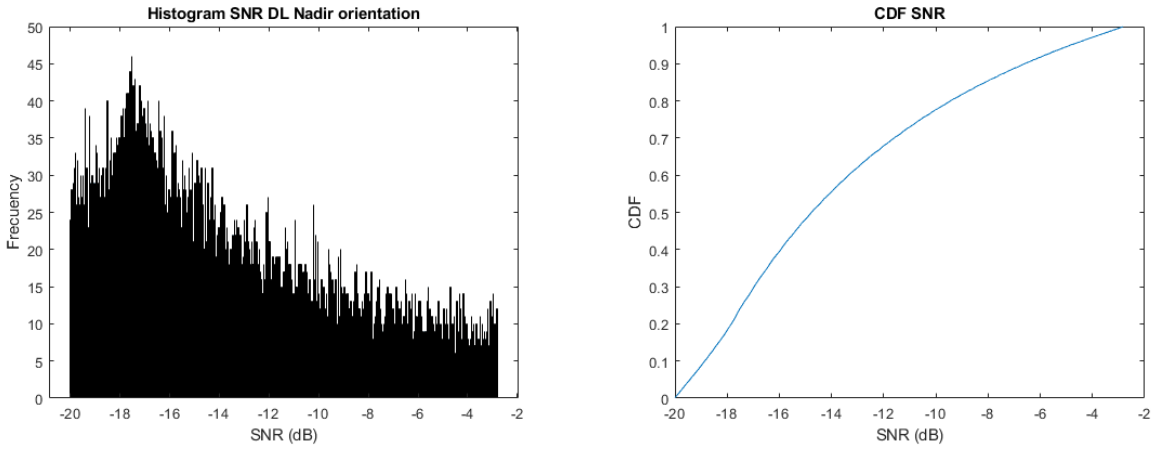

(a) (b)

Figure 29: SNR histogram (a) and SNR CDF (b) in DL scenario with Nadir orientation

An additional useful feature to study would be the contour lines, where the area covered by a given SNR range can be seen.

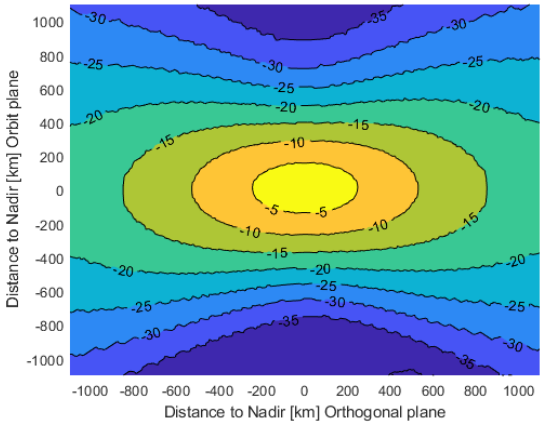

Figure 30: SNR heatmap with contour lines

The contour lines can be used to delimit the different SNR values, grouping them into clusters and calculating the coverage area for a certain SNR range. The following results were obtained.

Range	Area $[km^2]$
$SNR \geq -5(dB)$	116210
$SNR \geq -10(dB)$	476640
$SNR \geq -15(dB)$	1103900
$SNR \geq -20(dB)$	1683200

Table 9: DL Coverage area for one beam in the Nadir direction

Next, the uplink case has been characterized, obtaining the corresponding result.

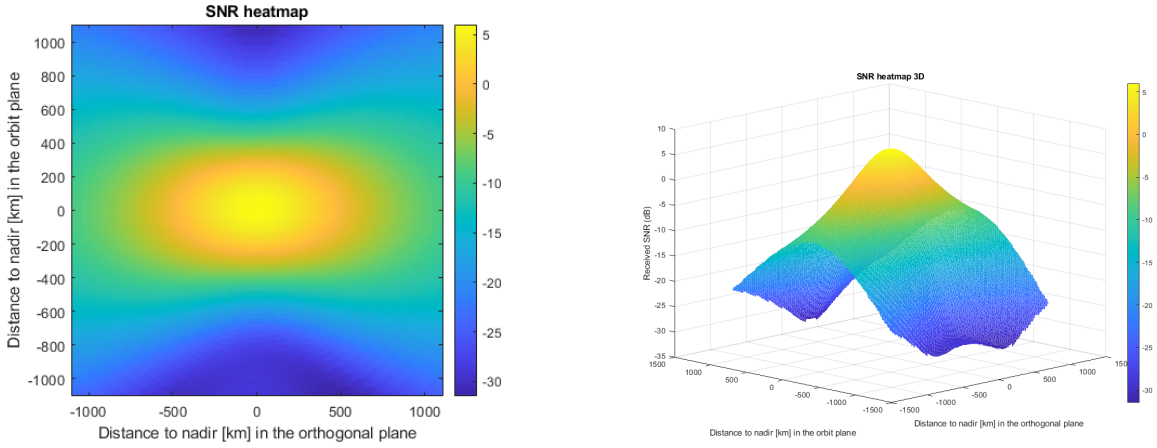

(a) (b)

Figure 31: SNR heatmap (a) and 3-D SNR heatmap (b) in UL scenario with Nadir orientation

And the following statistics:

Statistical parameter	Value
Total number of samples	28673
Mean	-9.1247
Minimum value (dB)	-19.9997
Maximum value (dB)	5.9974
Range	25.9971
Median	-9.296
Mode	5.986
Variance	42.2169
Standard deviation	6.4975

Table 10: Statistical values SNR UL for one beam in the Nadir direction

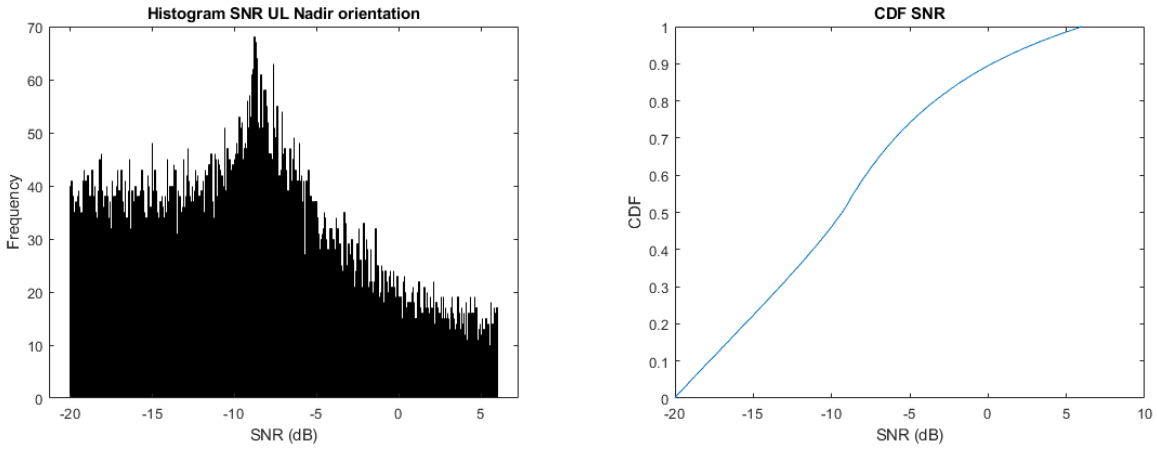

(a) (b)

Figure 32: SNR histogram (a) and SNR CDF (b) in UL scenario with Nadir orientation

Now, for the UL case, it will study the contour lines, where the area covered by a given SNR range can be seen.

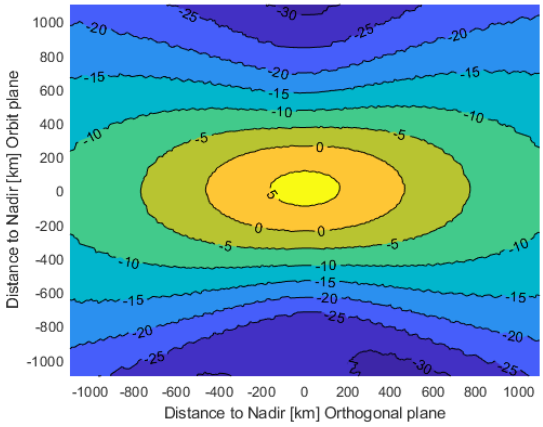

Figure 33: SNR heatmap with contour lines

The following results were obtained from the contour line.

Range	Area $[km^2]$
$SNR \geq 5(dB)$	52291
$SNR \geq 0(dB)$	373860
$SNR \geq -5(dB)$	917490
$SNR \geq -10(dB)$	1900600
$SNR \geq -15(dB)$	2730900
$SNR \geq -20(dB)$	3507400

Table 11: UL Coverage area for one beam in the Nadir direction

Regarding the study of the two scenarios, both DL and UL, the conclusion can be made that in the DL case it is limited in power, especially at the edges, while in the UL case it has a better result, this is due to the fact that in UL communications the bandwidth used is narrower so the noise would not affect as much as in the DL case. This improvement is observed of about $\approx$ 9dB dB. It should be noted that the noise figure in each case varies, in the case of NF in the satellite is 7 dBm while in the UE is 5dBm, this leads to better results in UL.

It is also observed how the coverage area increases, for -5dB it increases up to nine times more, in the UL scenario. The histogram and statistics show how the values improve considerably in the UL scenario.

3.3.1.1.5 Antenna direction to theta and phi angles

In this section it is added the functionality of modifying the orientation of the antenna to another location, this new position is described by two angles. These angles are θ and φ, which are defined in the following figure.

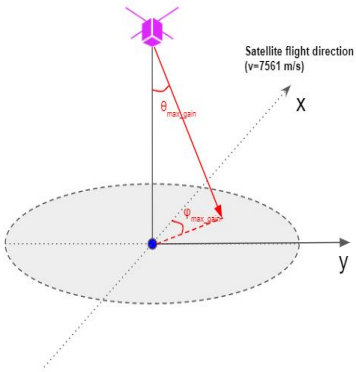

Figure 34: Characterization of the scenario where the antenna orientation is in term of θ and φ

The Euler's rotation theorem has been used to perform the orientation of the antenna. This theorem says that: any motion of a rigid body, in this case, the antenna, that keeps a constant point, must also leave constant a complete axis. This also means that any composition of rotations about a rigid body with arbitrary axes is equivalent to a single rotation about a new axis.

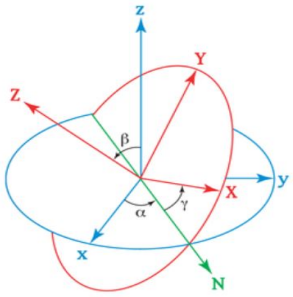

Figure 35: Euler's Rotation Theorem

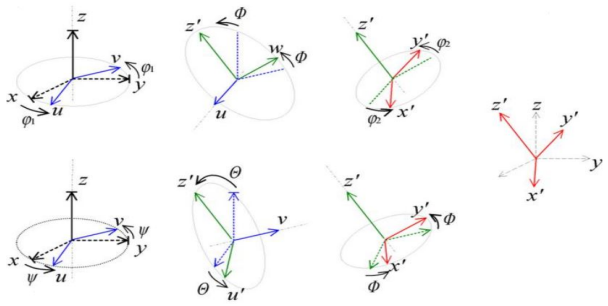

Figure 36: Euler's rotation theorem by phases

As shown in the figure, each time the antenna is rotated one axis remains stationary, so by rotating the correct angles (with the Euler matrices) it allows to orient the antenna to any point.

Finally it is possible to orient the radiation pattern of the antenna with the Euler rotation matrices.

The beam has been oriented towards $\theta = 45^o$ and $\varphi = 90^o$, resulting in the following radiation diagram as a function of the angles θ and φ and as a function of the angles γ_{orbit} and $\gamma_{orthogonal}$

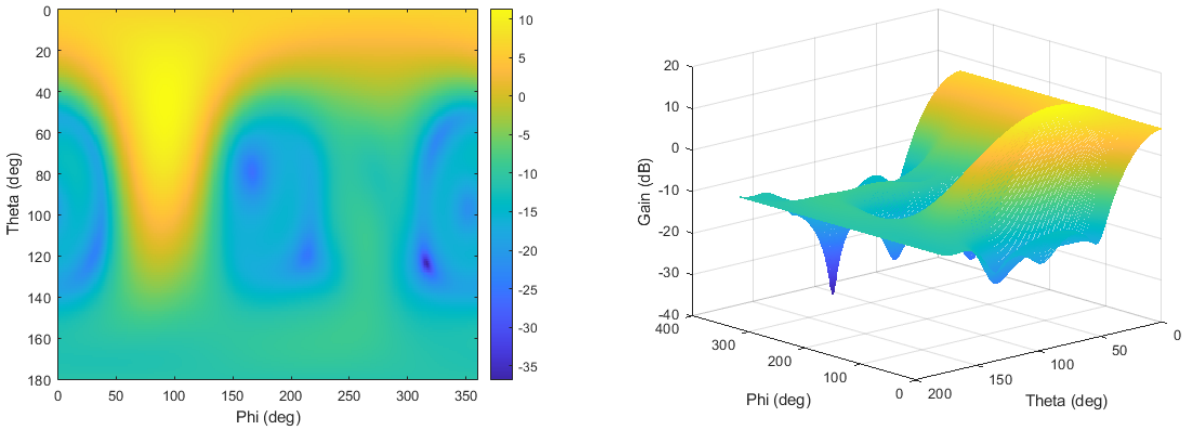

(a) (b)

Figure 37: Radiation pattern (a) and 3-D radiation pattern (b) in the scenario with a $\theta = 45^o$ and $\varphi = 90^o$ orientation in term of θ and φ

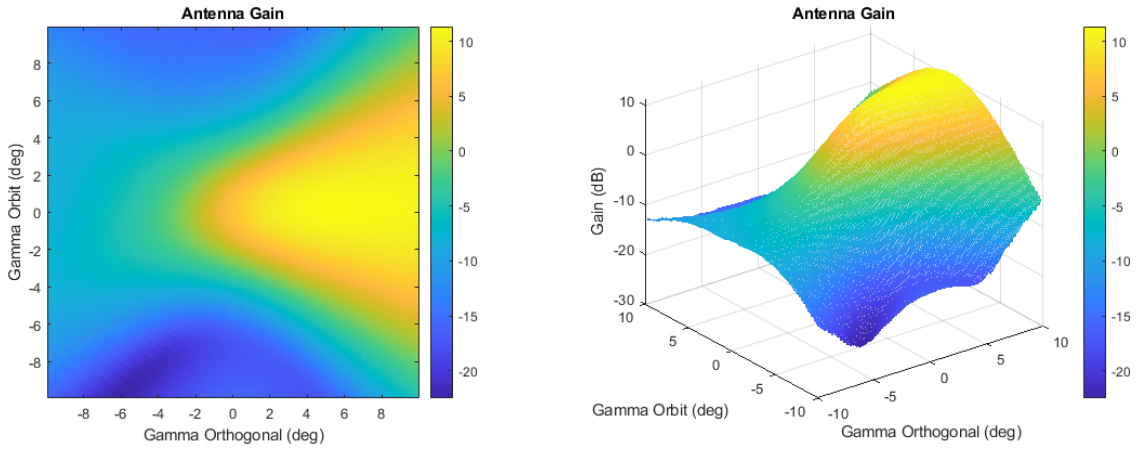

(a) (b)

Figure 38: Radiation pattern (a) and 3-D radiation pattern (b) in the scenario with a $\theta = 45^o$ and $\varphi = 90^o$ orientation in terms of γ_{orbit} and $\gamma_{orthogonal}$

With the rotated radiation pattern, it would already be pointing to the new orientation according to the angles described above, so inside the beam the values will be modified and the new SNR values can be obtained.

As analyzed in the previous case, the study of the heatmap and statistics will be separated for the DL and UL case.

In the first instance, the characterization has been performed for the downlink case obtaining the following result:

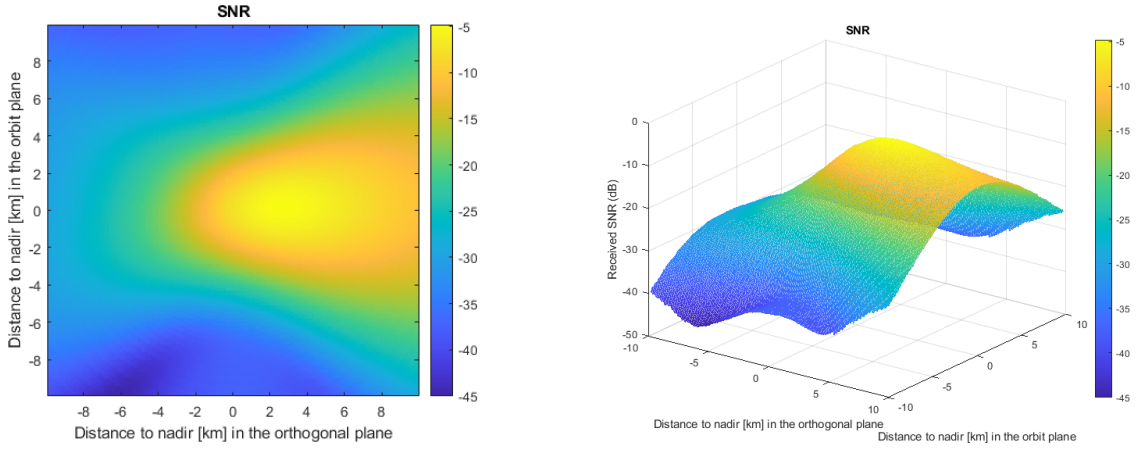

(a) (b)

Figure 39: SNR heatmap (a) and 3-D SNR heatmap (b) in DL scenario with with a $\theta = 45^o$ and $\varphi = 90^o$ orientation

With the following statistics:

Statistical parameter	Value
Total number of samples	13159
Mean	-12.59
Minimum value (dB)	-19.998
Maximum value (dB)	-4.7993
Range	15.2
Median	-12.3399
Mode	-7.6418
Variance	17.78
Standard deviation	4.216

Table 12: Statistical values SNR DL for one beam pointing to a certain direction

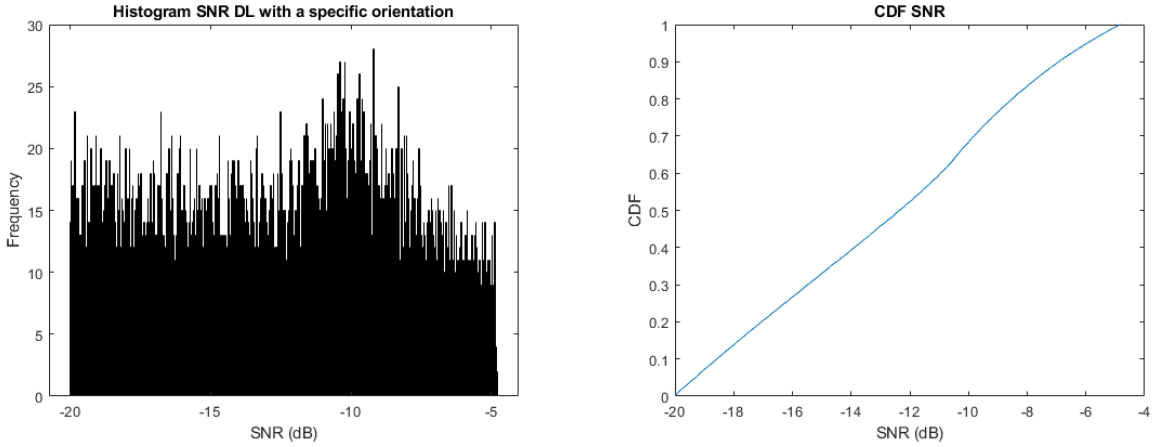

(a) (b)

Figure 40: SNR histogram (a) and SNR CDF (b) in DL scenario with a $\theta = 45^o$ and $\varphi = 90^o$ orientation

An additional useful feature to study would be the contour lines, where the area covered by a given SNR range can be seen.

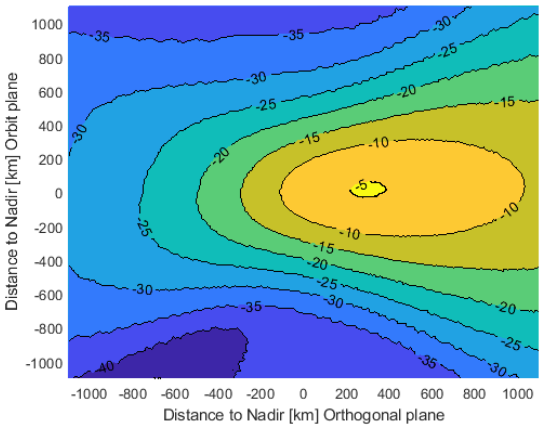

Figure 41: SNR heatmap with contour lines

The contour lines can be used to delimit the different SNR values, grouping them into clusters and calculating the coverage area for a certain SNR range. The following results were obtained.

Range	**Area** $[km^2]$
$SNR \geq -5(dB)$	11568
$SNR \geq -10(dB)$	476640
$SNR \geq -15(dB)$	1081000
$SNR \geq -20(dB)$	1610100

Table 13: DL Coverage area for one beam pointing to $\theta = 45^o$ and $\varphi = 90^o$ orientation

The uplink case has been characterized, obtaining the corresponding result.

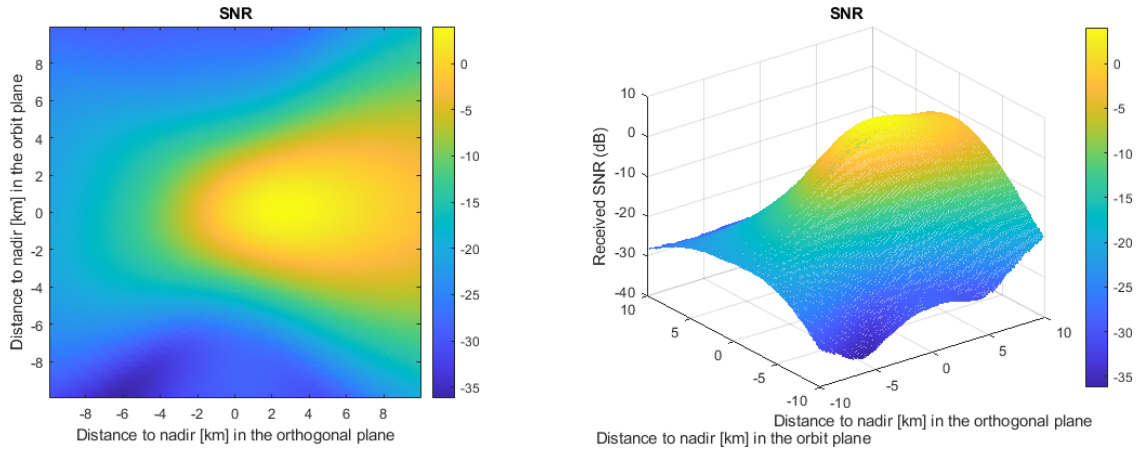

(a) (b)

Figure 42: SNR heatmap (a) and 3-D SNR heatmap (b) in UL scenario with a $\theta = 45^o$ and $\varphi = 90^o$ orientation

And the following statistics:

Statistical parameter	Value
Total number of samples	24305
Mean	-9.427
Minimum value (dB)	-19.999
Maximum value (dB)	4.013
Range	24.013
Median	-10.1
Mode	1.17
Variance	50.248
Standard deviation	7.089

Table 14: Statistical values SNR UL for one beam pointing to $\theta = 45^o$ and $\varphi = 90^o$ orientation

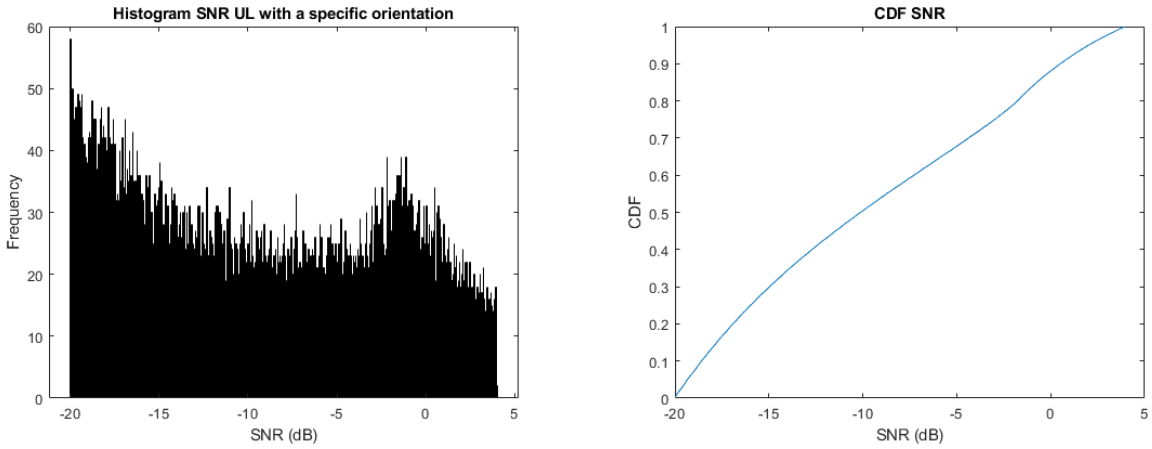

(a) (b)

Figure 43: SNR histogram (a) and SNR CDF (b) in UL scenario with a $\theta = 45^o$ and $\varphi = 90^o$ orientation

The area covered by a given SNR range can be seen in the contour line.

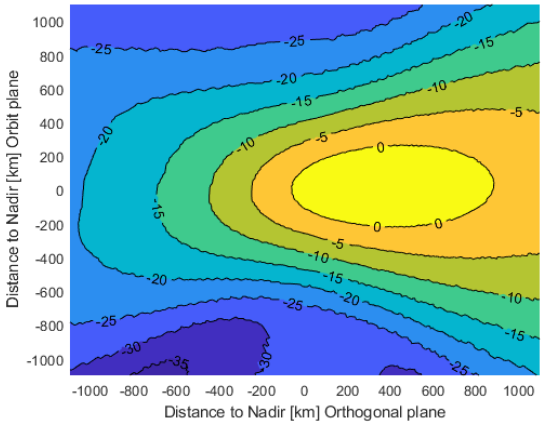

Figure 44: SNR heatmap with contour lines

The following results were obtained from the contour line.

Range	**Area** $[km^2]$
$SNR \geq 0(dB)$	360460
$SNR \geq -5(dB)$	960760
$SNR \geq -10(dB)$	1477400
$SNR \geq -15(dB)$	2092100
$SNR \geq -20(dB)$	2721100

Table 15: UL Coverage area for aone beam pointing to $\theta = 45^o$ and $\varphi = 90^o$ orientation

In this case, as in the previous case, the performance of the DL scenario is worse than that of the UL scenario, as mentioned above.

Another interesting case would be to compare the DL/UL scenario pointing to Nadir with the DL/UL scenario pointing at a certain angle.

Changing the tilt of the antenna for practical purposes, improves the pointing area, it would improve the mean, and the variance would be lower, the histogram that is observed is flatter, but if looking at the area, in the case of DL pointing towards Nadir, the area of -5 dB is much larger, this is because the distance is smaller, so there would be less losses and the SNR values are higher, but if looking at the area of -10dB it is exactly the same, so at global computation, it would have the same performance.

Comparing the UL scenarios, when the antenna tilt is changed the area improves a little, in this case, it does not have an area for SNR $\geq$ 5 dB but the area for SNR $\geq$ 0 dB is larger. This happens again with the area for SNR $\geq$ -15 dB.

3.3.1.1.6 Multiple beam

To conclude the study of the static scenario, the functionality of creating several beams has been added, this is achieved by adding several radio frequency systems to the satellite and orienting the antennas towards different points, thus increasing the satellite coverage and consequently providing service to a greater number of users with a single satellite. The scenario described would look like this:

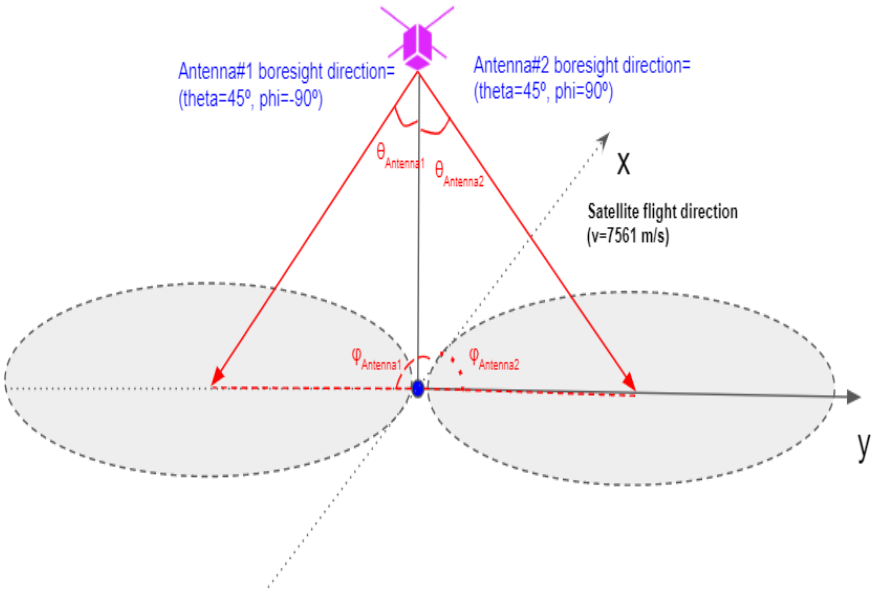

Figure 45: Characterization of multiple beam scenario

As there are two antennas, one beam is oriented in the direction $\theta = 45^o$ and $\varphi = 90^o$ and the other beam is oriented in the direction $\theta = 45^o$ and $\varphi = -90^o$. Obtaining the following radiation diagram as a function of the angles θ and φ and as a function of the angles γ_{orbit} and $\gamma_{orthogonal}$

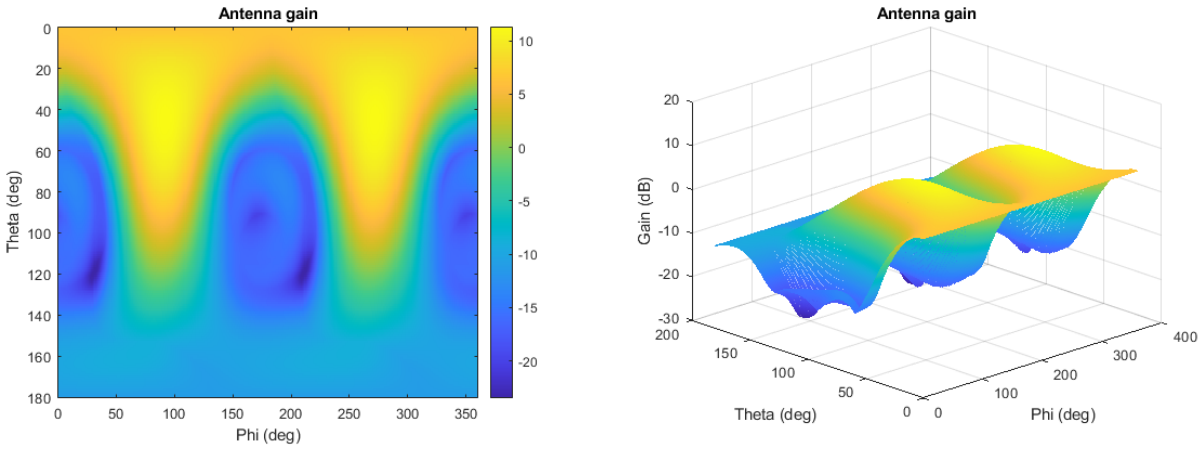

(a) (b)

Figure 46: Radiation pattern (a) and 3-D radiation pattern (b) in the scenario in the multiple beam scenario in term of θ and φ

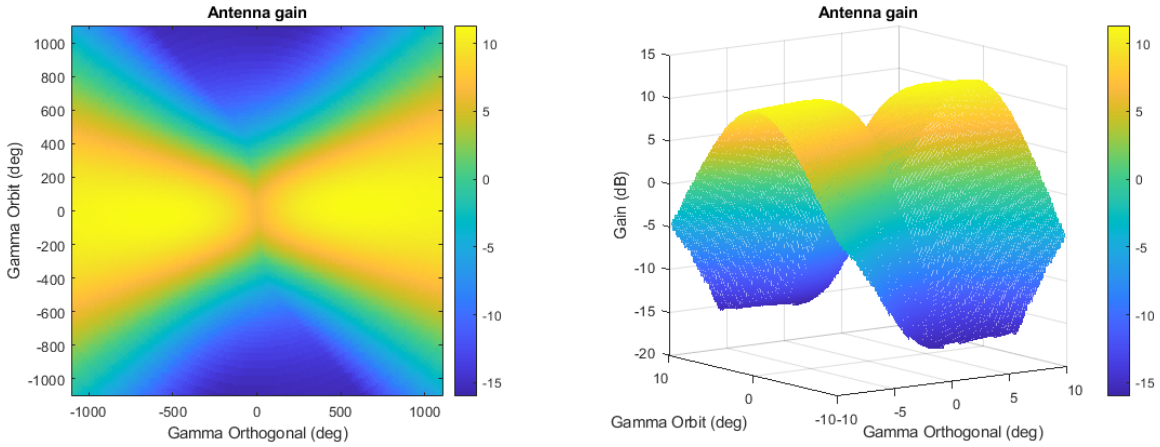

(a) (b)

Figure 47: Radiation pattern (a) and 3-D radiation pattern (b) in the multiple beam scenario in terms of γ_{orbit} and $\gamma_{orthogonal}$

As in the previous cases, the same study will be carried out for DL and UL. In the first instance, the characterization has been performed for the downlink case obtaining the following result:

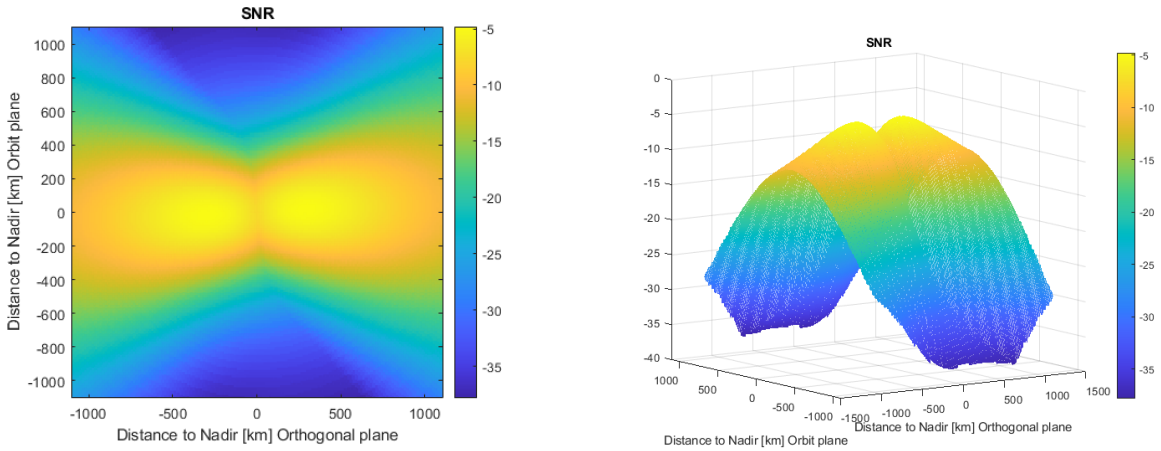

(a) (b)

Figure 48: SNR heatmap (a) and 3-D SNR heatmap (b) in the DL multiple beam scenario

With the following statistics:

Statistical parameter	Value
Total number of samples	21351
Mean	-11.94
Minimum value (dB)	-19.998
Maximum value (dB)	-4.7993
Range	15.2
Median	-11.399
Mode	-19.998
Variance	17.163
Standard deviation	4.143

Table 16: Statistical values SNR DL for multiple beams

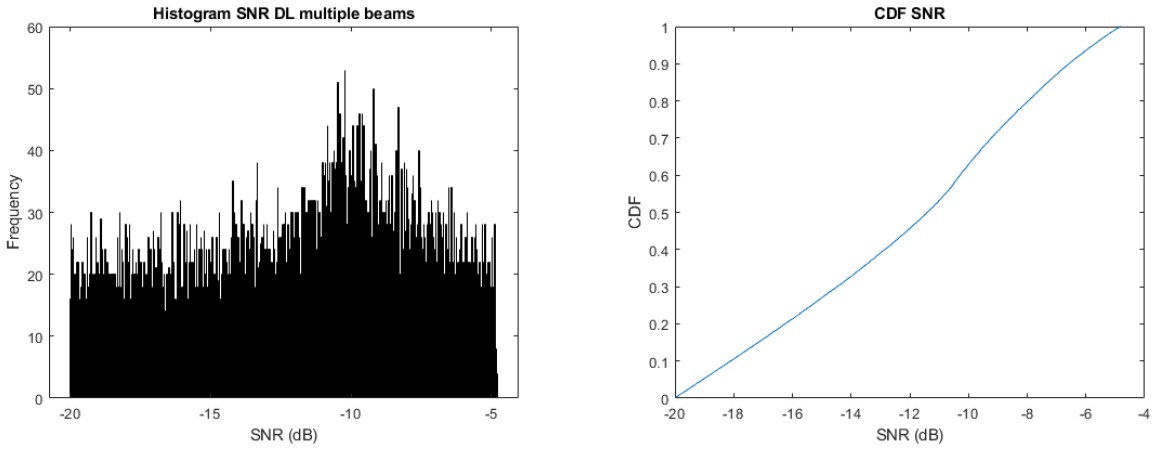

(a) (b)

Figure 49: SNR histogram (a) and SNR CDF (b) in the DL multiple beam scenario

The contour line will be presented.

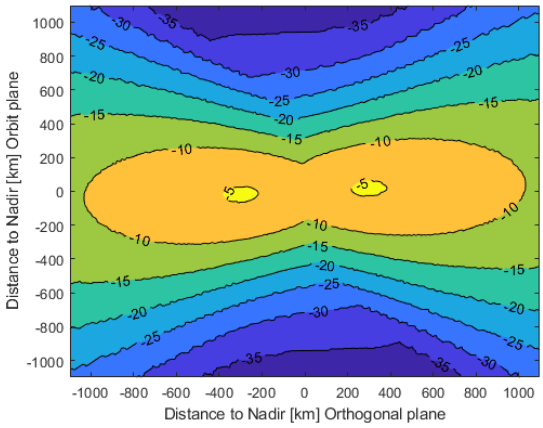

Figure 50: SNR heatmap with contour lines

With the following result:

Range	Area $[km^2]$
$SNR \geq -5(dB)$	2539.8
$SNR \geq -10(dB)$	979300
$SNR \geq -15(dB)$	1909100
$SNR \geq -20(dB)$	2611000

Table 17: DL Coverage area for multiple beams

Next, the uplink case has been characterized, obtaining the corresponding result.

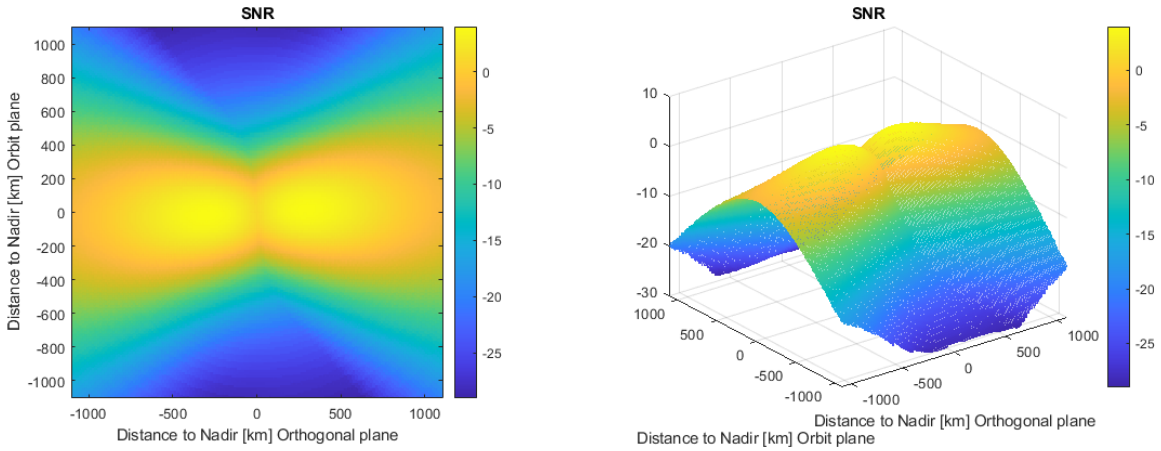

(a) (b)

Figure 51: SNR heatmap (a) and 3-D SNR heatmap (b) in the UL multiple beam scenario

And the following statistics:

Statistical parameter	Value
Total number of samples	30989
Mean	-6.994
Minimum value (dB)	-19.9996
Maximum value (dB)	4.0131
Range	24.01
Median	-6.096
Mode	-16.93
Variance	46.91
Standard deviation	6.849

Table 18: Statistical values SNR UL for multiple beams

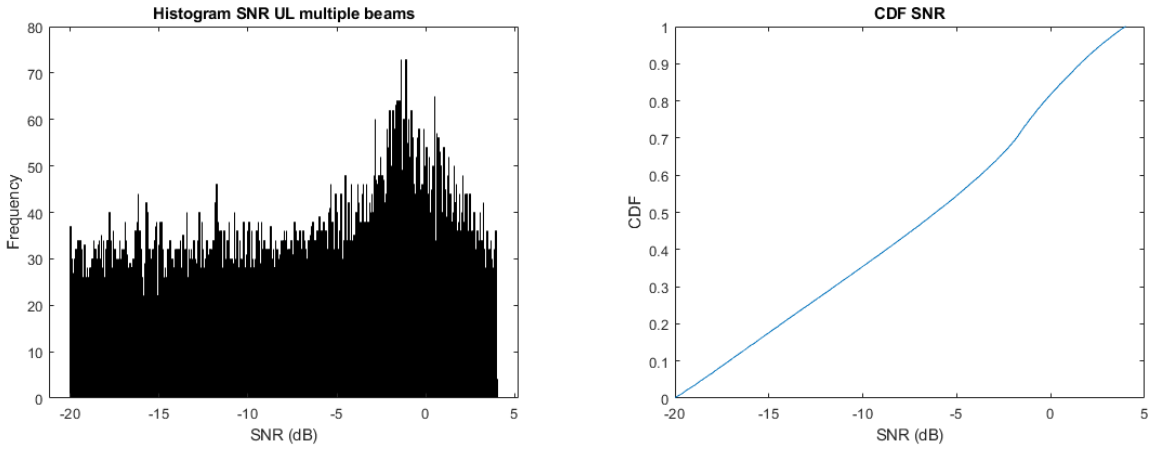

(a) (b)

Figure 52: SNR histogram (a) and SNR CDF (b) in the UL multiple beam scenario

Now, it will be presented the contour lines for this case.

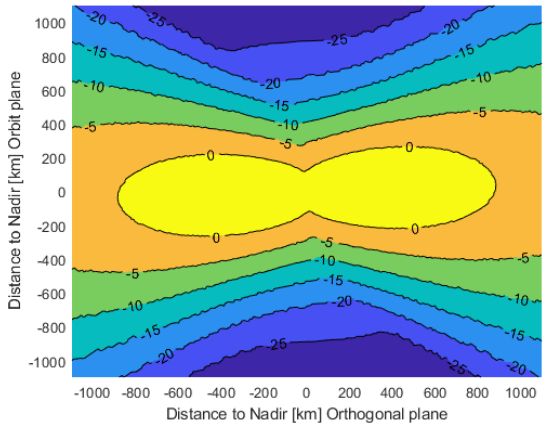

Figure 53: SNR heatmap with contour lines

With the following result for teach contour line.

Range	Area $[km^2]$
$SNR \geq -0(dB)$	701370
$SNR \geq -5(dB)$	1729400
$SNR \geq -10(dB)$	2449800
$SNR \geq -15(dB)$	3125400
$SNR \geq -20(dB)$	3274600

Table 19: UL Coverage area for multiple beams

In the case of adding two beams, it is obvious that the user's performance is improved, since two antennas are being used, In the case of DL, the area is doubled for all SNR ranges, except for the range greater than -5dB, where the area would be 4 times smaller, the rest of the range, the area is doubled.

In the case of UL, for high SNR ranges, the range is the double than in the scenario with one beam, but for low SNR ranges, the area is practically the same, even greater than in the scenario where the antenna tilt is modified.

3.3.1.2 Dynamic study

In this section a dynamic scenario will be studied, where the satellite is no longer in a static point over the earth and it is moving and making passes. An important aspect to characterize therefore would be the satellite pass, the view of the signal received from the device will depend on the maximum elevation angle that the UE has with the satellite. In addition, the satellite moves at a certain speed so it would be very useful to study the doppler effect that the device would receive, this effect will be explained in more detail in the following sections. Finally, it is also useful to characterize the delay that affects the signal as the satellite approaches and moves away from the terminal.

3.3.1.2.1 Characterization of a satellite pass (UL and DL SNR time evolution over a satellite pass

In the previous cases, it has been assumed that a snapshot of the satellite trajectory is taken as a reference when the satellite is pointing in the nadir direction. In these cases it would be a static situation. But to make it more realistic it is convenient to observe what happens when the satellite has a dynamic scenario, where it has a certain speed and is moving. This makes that the results seen by the NB-IoT device change over time.

The following scenario will be analyzed.

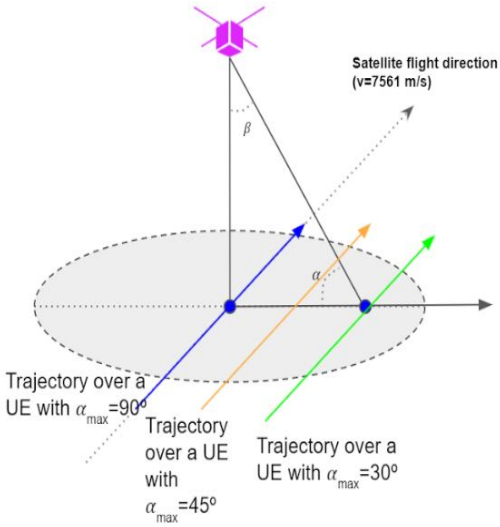

Figure 54: Characterization of scenario for satellite pass

The first case to be studied is how the SNR varies along the satellite pass. For this purpose a graph of how the SNR varies as the satellite approaches the UE or moves away from the UE will be shown. Measurements will be made for an angle $\alpha_{max} = 90$, .

In the following sections it will be studied how the SNR varies along the satellite pass, how the Doppler effect varies, or even how the propagation delay changes. For this purpose, several measurements will be made and it will be plotted how the SNR varies as the satellite approaches the UE or moves away from the UE. The same with the doppler effect and the delay propagation. These measurements will be made for several elevation angles, $\alpha_{max} = 90$, $\alpha_{max} = 45$ and $\alpha_{max} = 30$.

3.3.1.2.2 Variation of SNR as a function of elevation angle

The first case to be studied is how the SNR varies as a function of the satellite elevation angle along the satellite pass. For this purpose, several values of the elevation angle have been taken, as shown in figure (54).

This SNR value will depend directly on the elevation angle at which the UE sees the satellite. The simulation has been performed for $\alpha_{max} = 90$, $\alpha_{max} = 45$ and $\alpha_{max} = 30$. The plots show how the SNR value varies and how the elevation angle varies over the time.

The following graph shows how the value of the received signal varies as a function of the satellite elevation angle.

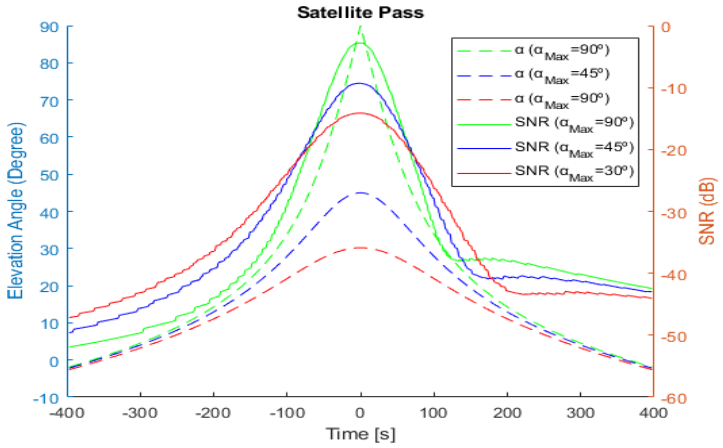

Figure 55: Variation of SNR as a function of elevation angle

The following results were obtained, for $\alpha_{max} = 90$ an SNR=-2.82 dB is obtained, for $\alpha_{max} = 45$ an SNR=-9.32 dB is obtained and for $\alpha_{max} = 30$ an SNR=-14.13 dB is obtained. It can be seen that there is a variation of up to $\approx$ 12 dB between a device with an elevation angle equal to 90^o and another with an angle equal to 30^o. There is a point at which for any α_{max}, the SNR value is $\approx$ -20 dB and that occurs after $\pm$70 s from the time it passes over the user in the nadir direction.

3.3.1.2.3 Doppler shift and Doppler shift Rate

When the satellite is in motion and the distance over time changes, the Doppler effect appears, this effect is described as the offsetting of the frequency of the signal transmitted between the satellite and the NB-IoT device. It is therefore extremely important to characterize this effect, to see what values it can take and how the frequency is shifted due to the Doppler from the central frequency.

For this reason, a plot of the Doppler shift variation during a satellite pass has been performed for a communication at a frequency of 2 GHz. Different results have been performed with different elevation angles in order to better characterize the scenario.

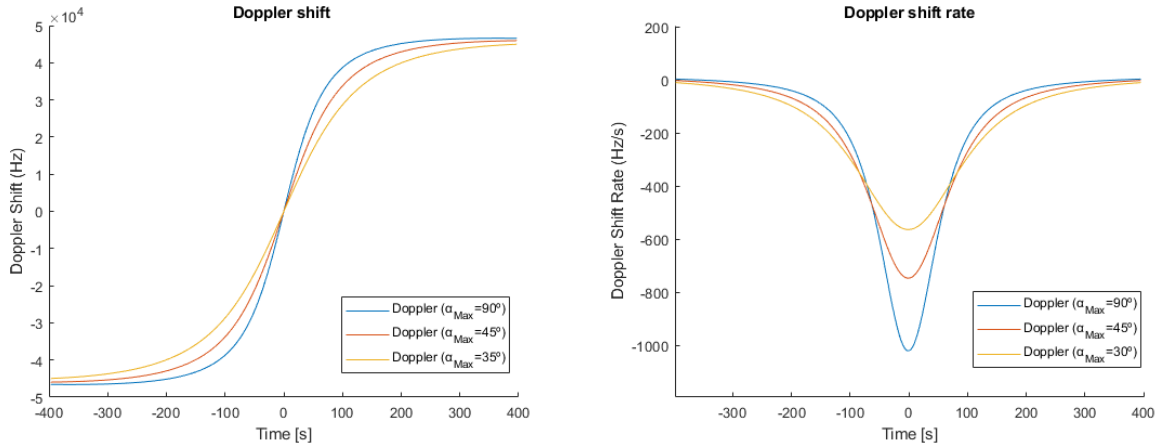

(a) (b)

Figure 56: Doppler shift (a) and Doppler shift rate (b) during a satellite pass

The maximum Doppler offset is ± 46kHz, this maximum is found when the satellite is flying far away towards the NB-IoT device, for different elevation angles very similar results are obtained.

Another important aspect is to see how this Doppler shift varies with time, i.e. how many hertz it varies per second, this new parameter is calculated as the derivative of the Doppler shift. The results are shown in the table presented above.

The maximum Doppler shift variation value occurs when the satellite is flying over the UE, this maximum value depends on the elevation angle, for $\alpha = 90$, the maximum value is 1021 Hz/s, for $\alpha = 45$, the maximum value is -747.4 Hz/s and for $\alpha = 30$ the maximum value is -564.2 Hz/s. It can be seen that the difference is $\approx$ 450 Hz/s between $\alpha = 90$ and $\alpha = 30$.

3.3.1.2.4 Propagation delay and propagation delay variation

The change of the distance from the satellite to the user, as well as causing a Doppler shift as seen in the previous chapter, also generates a propagation delay between the UE and the satellite, which varies as the satellite approaches or moves further away,

Therefore, it has been considered appropriate to plot this delay for different elevation angle and to study how it varies according to the position of the satellite.

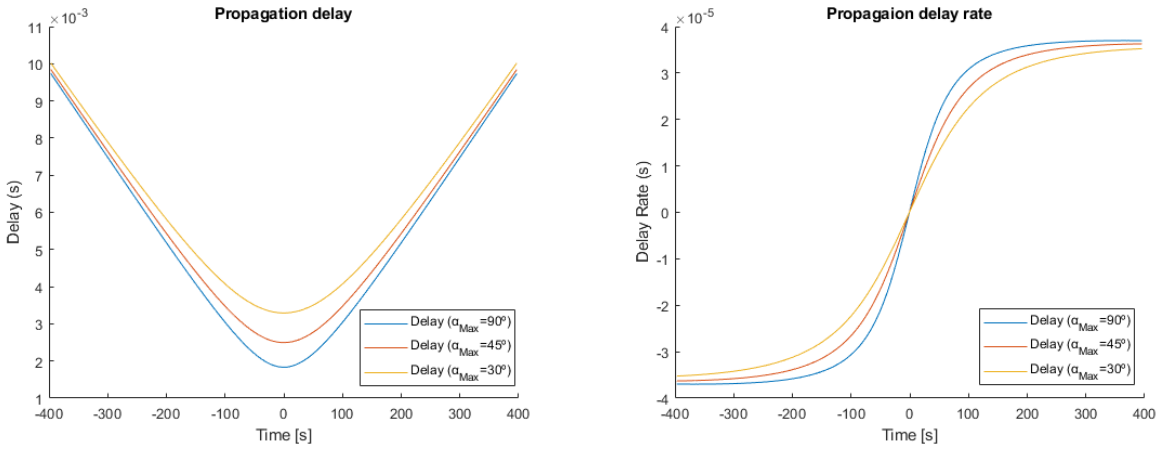

(a) (b)

Figure 57: Propagation delay (a) and propagation delay rate (b) during a satellite pass

The maximum propagation delay is about 10ms when the satellite is far away from the UE, when the satellite is flying over the NB-IoT device, the propagation delay depends on the elevation angle of the satellite, for $\alpha = 90$, the maximum value is 1.8 ms, for $\alpha = 45$, the maximum value is 2.5 ms and for $\alpha = 30$ the maximum value is 3.3 ms. This implies a delay difference of 1.4 ms between $\alpha = 90$ and $\alpha = 30$.

In addition, it has also been considered to study how this delay varies over time, for this purpose the derivative of the propagation delay has been calculated, it has been called propagation delay variation. The results are shown in the table presented above.

The maximum propagation delay rate is 36 $\mu s/s$ when the satellite is far away from the UE.

4 Link level performance analysis

This chapter provides an assessment of the operation of the NB-IoT protocol by means of link level simulations. In particular, the minimum SNR needed to achieve a target BLER is estimated for different satellite link models and configuration options of the protocol (MCS, TBS, repetitions). Achievable spectral efficiency is also estimated.

First, the models of the scenario being simulated are described, both the transmission and reception models used and the type of channel involved in the process, as well as the different channel estimator models used. Finally, the performance of the simulations carried out in this section are presented.

4.1 Transmission and reception modelling

In this section it will be studied how both the transmitter and the receiver have been modeled. For these models the transmitter and receiver models that MATLAB has created for the following examples have been used: NB-IoT NPDSCH Block Error Rate Simulation and NB-IoT NPUSCH Block Error Rate Simulation.

In the case of DL data transmission, first a transport block (TB) with a predetermined size and a random bit stream is created, this TB is subjected to CRC coding, convolutional coding and rate adaptation in order to obtain the NPDSCH bits.

These bits can be repeated depending on the value of the variable subframe repetition.

To form the NPDSCH complex symbols, the bits are coded, modulated, layer mapped and precoded. These complex symbols are mapped onto the network and modulated using OFDM to create the time domain signal.

The signal is then passed through the channel and an AWGN noise is added.

The received signal is synchronized and demodulated, then channel estimation and equalization is performed to recover the NPDSCH symbols, after which channel decoding and demodulation is performed to recover the transport block.

If repetition has been used, the repeated subframes are combined before rate recover.

Finally for each SNR the transport block error rate is calculated.

A more illustrative view of all the processes that are carried out is presented in the following diagram.

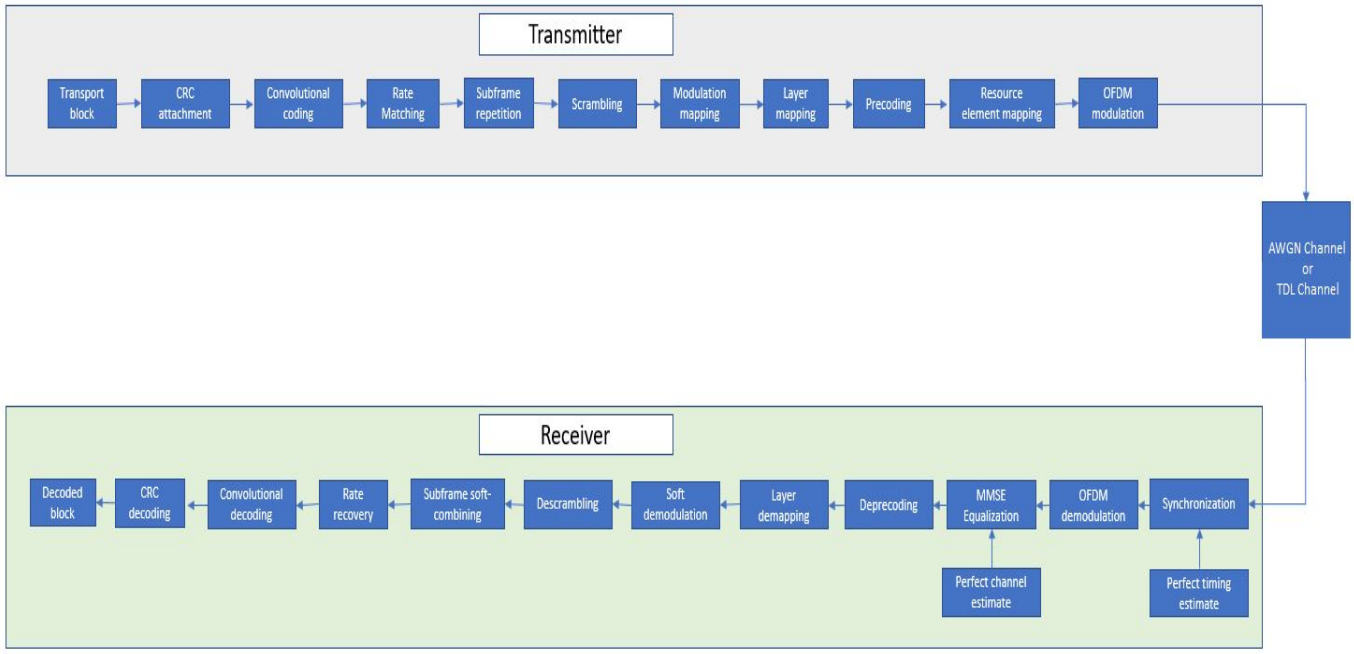

Figure 58: Description of the NPDSCH transmission and reception model

For the case of UL data transmission, in the case that the processing is carried out using format 1, which would be the format where data is sent and which has been used in this analysis,

First, a stream of random bits is generated and incorporated in a transport block of a specific size. Then, CRC coding, turbo coding and rate adaptation are performed to create the NPUSCH bits. After, interleave the bits per resource unit to apply a time mapping first and create the NPUSCH code word.

Afterwards, the coding, modulation, layer mapping and precoding are performed in the codeword to form the complex NPUSCH symbols and then assign the NPUSCH symbols and the corresponding DRS to the resource grid.

Then, the time domain waveform is generated by SC-FDMA modulation of the resource network and pass the waveform through an AWGN channel or TDL channel depending on the case to be studied.

Finally to recover the transmitted signal, synchronization, channel estimation and MMSE equalization are performed, the NPUSCH symbols are extracted and the transport block is recovered by demodulating the symbols and decoding the channel with the resulting bit estimates.

4.2 Channel modelling (AWGN, TDL channel, Doppler due to satellite velocity)

This section will explain how the different channels have been modeled, both AWGN and tapped delay line (TDL), as well as the most important features to be taken into account in NTN communications, such as the different Doppler effects.

4.2.1 Channel AWGN

The Gaussian channel is used to model the wide range of real cases in communications, it is considered as an ideal channel, whose impulse response in frequency is flat, which means that its impulse response fulfills that $|h| = 1$. When the signal travels through the channel it is when an additive white Gaussian noise is added to it.

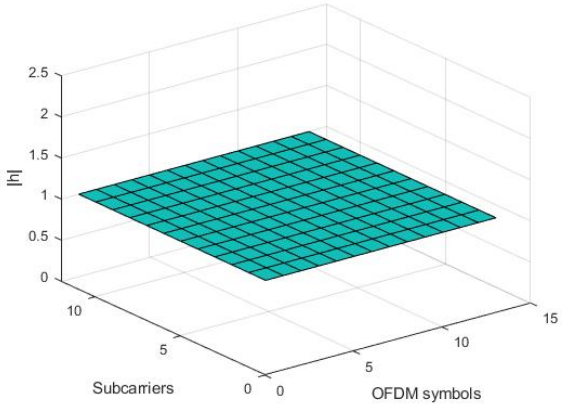

Figure 59: Impulse response AWGN channel

Therefore, the received signal will only be affected by the AWGN noise, since the channel will not incorporate attenuation or fading. The received signal at the receiver will be $r(t) = s(t) + n(t)$. Where $r(t)$ is the received signal, $s(t)$ is the transmitted signal and $n(t)$ is the noise signal.

The noise amplitude would be calculated as a function of SNR and would be calculated according to the following equation:

$$N_0 = \frac{1}{\sqrt{2 \cdot N_{FFT}} \cdot SNR} \tag{19}$$

Resulting in a noise power such that:

$$P_{noise} = |N_0|^2 + |N_0|^2 = \frac{1}{N_{FFT} \cdot SNR^2} \tag{20}$$

Assuming that the power of the signal is

$$P_{tx} = \frac{P_{sc}}{N_{FFT}^2} \cdot 12 \tag{21}$$

Then the received power is

$$P_{rx} = P_{tx} + P_{noise} = N_{FFT} \cdot (\frac{12}{N_{FFT}} + \frac{1}{SNR^2}) \tag{22}$$

To create the additive white Gaussian noise, N_0 is multiplied by a random vector of complex numbers of the size of the received signal.

4.2.2 Channel TDL

To study the scenario in a more realistic way, it is necessary to take into account that the channel is not an AWGN channel model because there are echoes of the transmitted signal due to reflections with buildings or objects in the environment. For a more accurate study of the channel, it has been proposed to model it with a tapped delay line (TDL) channel, in order to be able to characterize these effects better. This channel is defined as several components, the first component follows a Rician distribution, it corresponds to the first tap, which will be line of sight (LOS) path, this case occurs when there is a direct path that is not reflected by any obstacle between the transmitter and the receiver. The Probability Density Function (PDF) of Rician distribution is given by the following equation:

$$f_{\text{Rician}}(r|\nu,\sigma) = \begin{cases} \frac{r}{\sigma^2}\exp\left[\frac{-(r^2+\nu^2)}{2\sigma^2}\right] \mathrm{I}_0\left(\frac{r\nu}{\sigma^2}\right) & \text{for } r \geq 0 \\ 0 & \text{otherwise} \end{cases}$$

Figure 60: Probability Density Function (PDF) of Rician distribution

Where I_o is the modified Bessel function. The following taps would follow a Rayleigh distribution corresponding to the non-light of sight (NLOS) components, in this case each path is reflected by objects at least once between the transmitter and receiver. The Probability Density Function (PDF) of Rayleigh distribution is given by the following equation:

$$f_{\text{Rayleigh}}(r|\sigma) = \begin{cases} \frac{r}{\sigma^2}\exp\left[-\frac{r^2}{2\sigma^2}\right] & \text{for } r \geq 0 \\ 0 & \text{otherwise} \end{cases}$$

Figure 61: Probability Density Function (PDF) of Rayleigh distribution

The impulse response of the channel can be modeled with the following equation.

$$\mathrm{h}(\mathrm{t},\tau) = h_0(\tau)\delta(\tau) + \sum_{k=1}^{K-1} h_k\delta(\mathrm{t}-\tau_k)$$

Figure 62: TDL model equation

Where K corresponds to the number of fading channel paths, the term h_o is the coefficient of the first tap, while the values h_k and τ_k corresponds to the coefficients and delays of the k^{th} path, respectively.

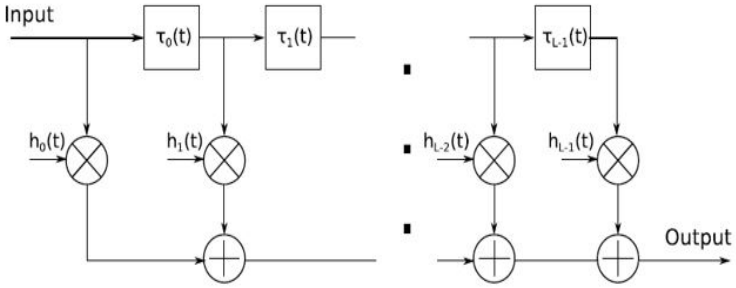

Figure 63: TDL channel system model

The TDL channel considered in this study has a Rician component, which corresponds to the LOS path, and two Rayleigh components. All the values are shown in the following table [16]:

Number of Tap	Normalized delay	Power in [dB]	Fading distribution
1	0	-0.394	LOS path
1	0	-10.618	Rayleigh
2	14.8124	-23.373	Rayleigh

Table 20: TDL channel model

The first tap follows a Rician distribution with a K-factor of $K_1 = 10.224dB$ and a mean power of 0 dB.

4.2.3 Doppler effects

To model the New Radio (NR) non-terrestrial network (NTN) channels, in addition to using a frequency selective fading tapped delay line (TDL) channel. This channel only generates path gains following the distribution that has been configured. But in order to correctly characterize an NTN connection, the Doppler effect must be applied.

The Doppler effect consists of the variation in the wavelength of any type of wave emitted or received by a moving object. This effect is perceived by the receiver as a frequency shift. The main cause of the effect in the scenario is the relative motion between the satellite and the UE. This is due to the fact that the scenario studied is a communication between a satellite that is in a LEO orbit, which has an orbital period of about 100 minutes and a very high satellite speed.

In this case there are two different Doppler effects, one corresponds to the Doppler shift due to the satellite movement and the other is the Doppler shift due to the user movement.

The Doppler shift due to satellite motion depends on the satellite velocity, satellite orbit (satellite height), elevation angle and carrier frequency. This Doppler shift is calculated as [13]:

$$f_{d,sat} = (\frac{v_{sat}}{c}) \cdot (\frac{R_E}{R_E + h_s} \cdot \cos(\alpha)) \cdot f_c) \tag{23}$$

Where

- v_{sat} is the velocity of the satellite.
- c is the speed of light.
- R_E is the radius of the Earth.
- h_s is the altitude of the satellite.
- α is the elevation angle of the satellite.
- f_c is the carrier frequency.

This formula is only valid when the satellite passes over the device, therefore by applying the sine theorem between the angles α and θ the following equation can be obtained, valid for any satellite trajectory and the device can be at any point within the beam.

$$f_{d,sat} = (\frac{v_{sat}}{c}) \cdot \sin(\theta) \cdot \cos(\varphi) \cdot f_c \tag{24}$$

The demonstration is as follows:

$\frac{h_s}{\sin(\theta)} = \frac{R_E + h_s}{sen(\alpha + 90)}$

$\cos(\alpha) = \frac{R_E + h_s}{h_s} \cdot \sin(\theta)$

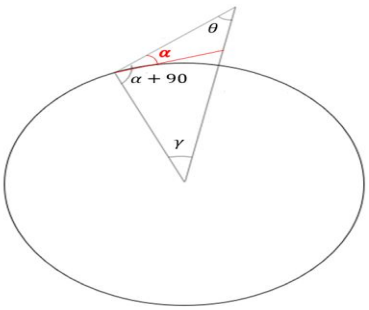

Figure 64: Overview of the angles on the scenario

To apply this Doppler effect to the signal, the signal has been multiplied by a complex exponential as follows:

$$x(t) = s(t) \cdot e^{-2\pi \cdot f_{d,sat} \cdot t} \tag{25}$$

In addition, the correct performance of the Doppler effect simulation due to the movement of the satellite has been checked in a graphical way, seeing how the frequency spectrum of the generated signal varies.

On the other hand, there is also the Doppler due to the motion of the UE. This Doppler spectrum for each tap is characterized by a classical (Jakes) spectrum and a maximum Doppler shift f_D. [20]

The equation is:

$$f_D = \frac{|\bar{v}|}{\lambda_0} \tag{26}$$

The Doppler spectrum additionally contains a peak at the Doppler shift $f_s = 0.7 \cdot f_D$ with an amplitude such that the result of the fading distribution has the specified K-Factor.

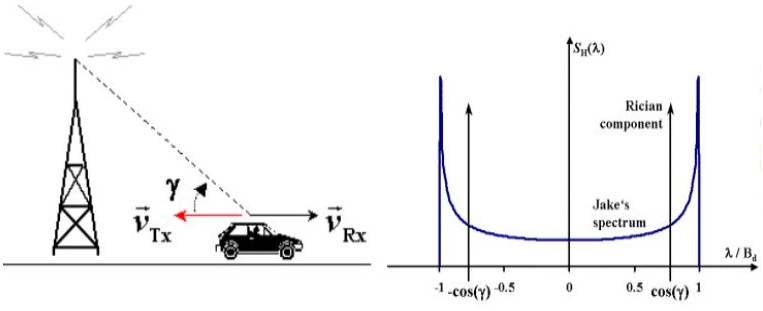

Figure 65: User mobility scenario and Jake's spectrum

To summarize and to see in a graphical way, both Doppler, the Doppler effect due to the satellite motion and the Doppler effect due to the UE motion, the following picture is presented:

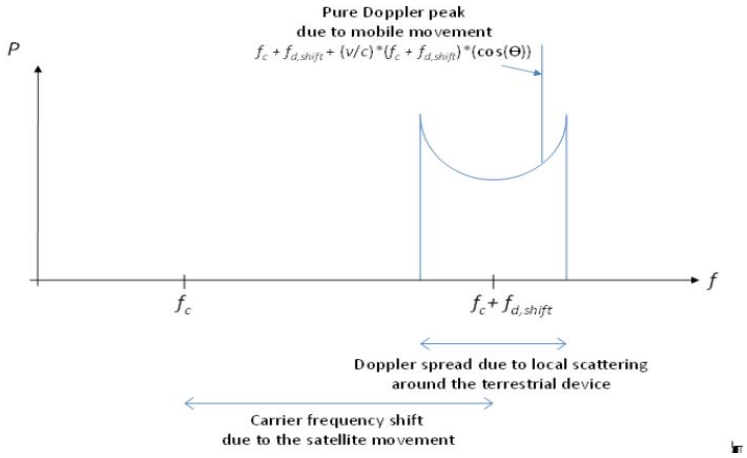

Figure 66: Doppler power spectrum in NTN in LOS conditions

In order to verify the frequency peak that appears in f_s, several simulations have been performed, where some parameters have been modified, such as the frequency, Doppler frequency due to the satellite motion or the Doppler frequency due to the UE motion.

Therefore, it has been checked visually and mathematically how the equation $f_s = 0.7 \cdot f_D$ is fulfilled.

The values used are shown in the following table.

f (Hz)	10	10	10	10	10	10	10	10	10	10
$f_{d,sat}$ (Hz)	5	5	5	5	5	5	5	5	5	5
f_c (Hz)	15,5	16,5	17	18	18,5	19	20	20,5	21,5	22
f_D (Hz)	1	2	3	4	5	6	7	8	9	10
f_s (Hz)	0,5	1,5	2	3	3,5	4	5	5,5	6,5	7
$\frac{f_s}{f_D}$ (Hz)	0,5	0,75	0,66	0,75	0,7	0,66	0,71	0,68	0,72	0,7

Table 21: Doppler effect testing

It can be seen how it always uses an angle of 45^{o} for the angle of incidence of the Rice component ($\cos(45^o) = 0.7$).

4.3 Channel estimator

In order to be able to recover the information sent when it arrives at the receiver, it is necessary to estimate the channel over which the data has been transmitted, so the performance of the system can be improved.

A channel estimator determines a channel estimate of a wireless communications channel based on a signal received over the wireless channel.

In this study two types of channel estimators are going to be seen, one would be the perfect channel estimator and the other would be a more practical channel estimator, both will be described below.

The perfect channel estimator is able to estimate the entire channel grid, exactly as it is. The estimation function first reconstructs the channel impulse response from the channel path gains and the path filter impulse response. The function then performs the OFDM demodulation for number of resource blocks with subcarrier spacing and initial slot number. As it can be seen, this perfect estimator estimates the channel perfectly.

On the other hand, the practical estimator is a Pilot Aided, P/A estimator. The PA estimation uses known pilots to obtain the channel information. The pilot information consists of certain symbols that are known in the data transmitted at predetermined locations on the time-frequency grid. Therefore, the transmitter sends such pilot information along with the useful signal. In the receiver will be performed the estimation of the pilot signals information. Once the estimator extracts the information contained in the pilots, it is necessary to know the channel response over the entire grid, for which different interpolation schemes are used. This estimator uses a cubic interpolator and then it

uses an LSE estimator with the help of the eNB information to complete the following interpolated points.

A useful way to check that the practical channel estimator performs all the above processes is to be able to see it graphically. For this purpose, scenarios with variable Doppler and for a fixed SRN are presented, where both estimators can be observed. The Doppler effect has been added so that the channel has a curvature and the estimator can be further examined.

In order to better understand the practical channel, it is first presented how the values of the NRS pilot signal would be distributed on the grid [17].

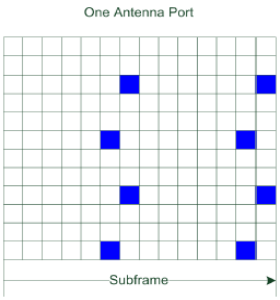

Figure 67: Basic mapping of reference signals to the resource elements

Once the location of these signals is known, it is easier to visualize how the practical estimator works, for this purpose, the following pictures will be presented:

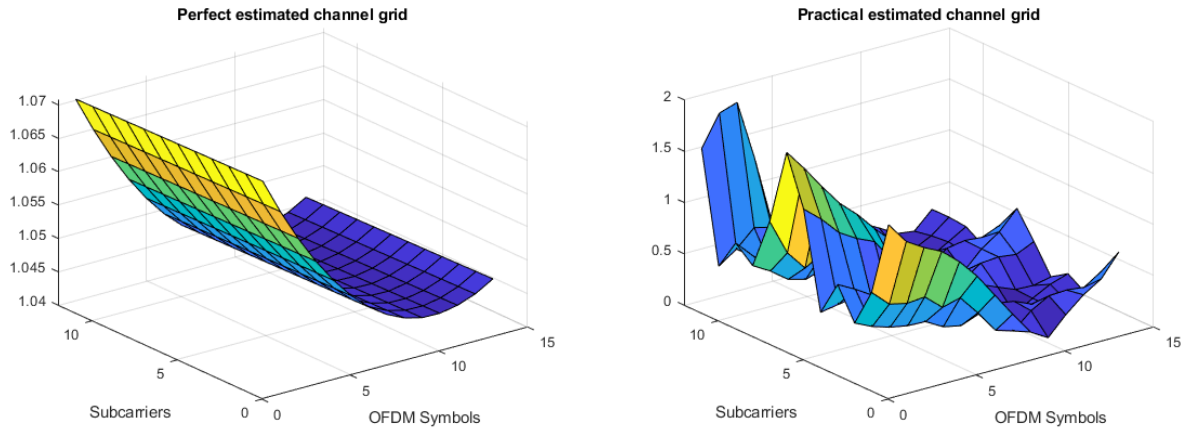

(a) (b)

Figure 68: Perfect channel estimator for Doppler = 100 Hz (a) and practical channel estimator for Doppler = 100 Hz (b)

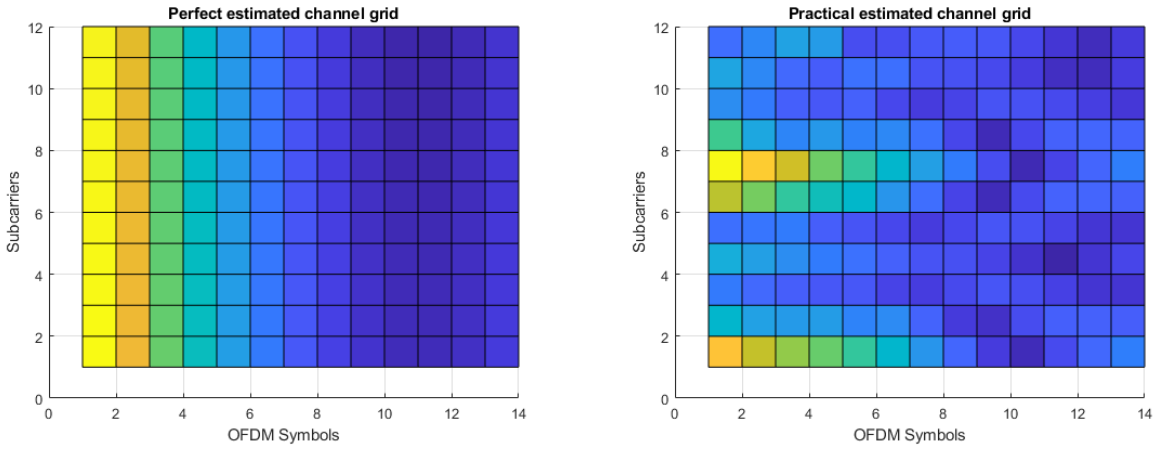

(a) (b)

Figure 69: Perfect channel estimator for Doppler = 100 Hz (a) and practical channel estimator for Doppler = 100 Hz (b)

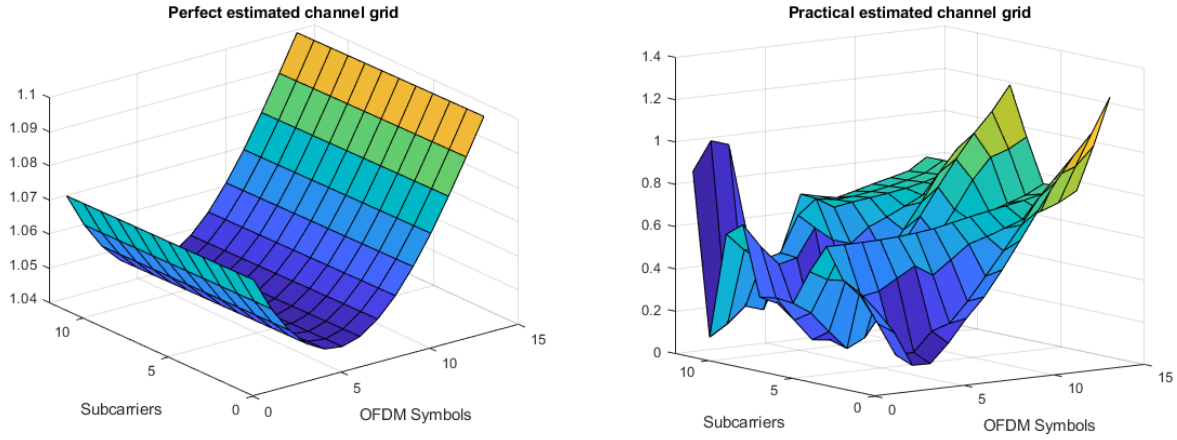

(a) (b)

Figure 70: Perfect channel estimator for Doppler = 200 Hz (a) and practical channel estimator for Doppler = 200 Hz (b)

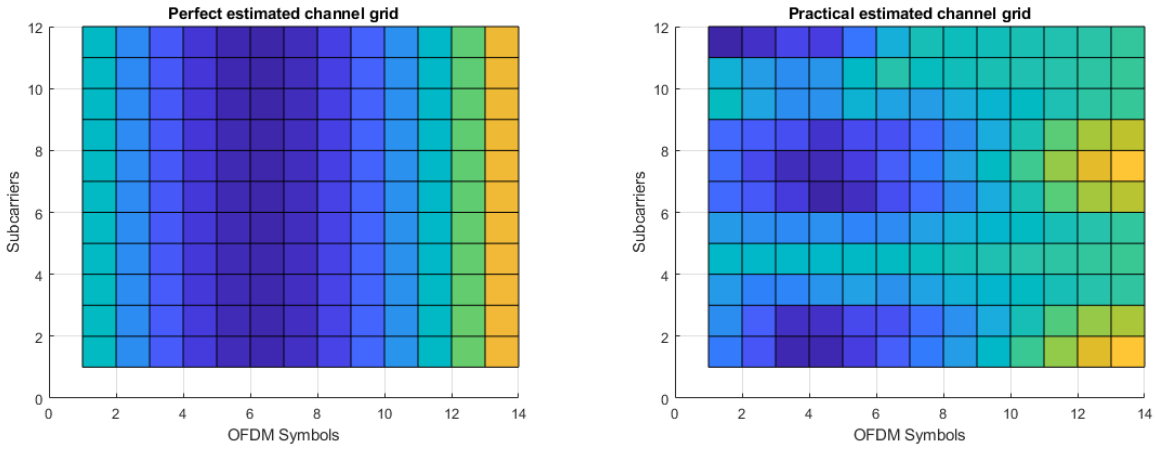

(a) (b)

Figure 71: Perfect channel estimator for Doppler = 200 Hz (a) and practical channel estimator for Doppler = 200 Hz (b)

With these images, it is possible to see how in the zones where the NRS signals and their contiguous symbols are located, the channel is very well estimated, it can be observed that the practical estimator fulfills this function.

4.4 Performance results (SNR / Espectral efficiency for different channel/transmission/reception configurations)

In this section the results of the different simulations that have been carried out in the study are shown, both for the downlink and uplink cases. All the analysis has been performed in order to have a QoS (Quality of Service) of the system that guarantees a BLER no higher than 10%. Under this requirement, the communication between satellite and device works properly and the service provided by the device is not altered by channel impairments [11].

4.4.1 NB-IoT NPDSCH performance

In order to start, it would be necessary to choose the amount of transport block to simulate, because it is possible to perform a simulation with a variable number of TB, for this purpose two variables have been defined. T_{Frag} and N_{Frag}, being fragment duration (measured in TB) and number of fragments respectively.

This allows to fix a number of fragments of a given duration, instead of considering a continuous time interval, in order to be able to estimate the average value before.

In addition, the idea of performing multiple simulations is to be able to characterize two effects:

1. The effect of the Gaussian noise, which is additive and changes subframe by subframe.

2. The effect of the propagation channel which, in the case of the TDL channel, means that the channel attenuation is a Rice variable which, for low Doppler, can be kept invariant throughout a single simulation.

To take into account the first point, as the intention is to obtain SNR where the system shows a BLER=10% (i.e. for every 10 TBs send on average one is erroneous), it would be enough to simulate an interval where on average 500 erroneous blocks are obtained, therefore 5000 TBs should be simulated, therefore 5 seconds of simulation (assuming that 1 TB is transmitted in 1 SF). In this case, fragmentation will be performed.

To take into account the second point, several split simulations are performed in small values in order to have several realizations of the variable Rice, so in each interval a different value of Rice is used.

The objective is to calculate the number of simulations needed to obtain a BLER standard dispersion of less than 3% for a fixed value of SNR and therefore also to characterize the behavior of the Rice variable.

Values of N_{Frag} and T_{Frag} will be chosen that are equal in both DL and UL scenarios and that both meet the condition of less than 3% dispersion.

For this purpose, the value of T_{Frag}=100 TB is set and the optimal value of N_{Frag} is calculated. It should be noted that in each N_{Frag} the value of the channel seed is different. With this, the unknown behavior of the channel is averaged in order to obtain changes in the channel response (TDL channel) and thus to better characterize all the variability of the channels until it is grouped near a value, this variability is the one that will be studied with the standard dispersion.

For each scenario, 50 simulations have been performed in order to properly characterize the experiment and to extract the corresponding statistics.

The statistics to be taken into account are:

- BLER average
- Maximum BLER
- Minimum BLER
- Standard deviation, it will be computed using the following formula, with N=50.

$$\sigma = \sqrt{\frac{\sum_{i=1}^{n}(x_i - \bar{x})^2}{N}} \tag{27}$$

The results are the following:

$N_{Frag} = 50$				
	Mean	**Maximum**	**Minimum**	**Standard deviation**
AWGN	9.66%	10.72%	8.44%	0.44%
TDL 1	9.16%	16.4%	2.44%	3.23%
TDL 2	9.95%	12.84%	7.80%	1.03%
TDL 3	9.62%	11.08%	8.02%	0.62%
$N_{Frag} = 100$				
	Mean	**Maximum**	**Minimum**	**Standard deviation**
AWGN	9.69%	10.39%	9.06%	0.32%
TDL 1	9.63%	16.73%	5.47%	2.57%
TDL 2	9.76%	12.21%	8.28%	0.78%
TDL 3	9.59%	10.67%	8.2%	0.5%
$N_{Frag} = 200$				
	Mean	**Maximum**	**Minimum**	**Standard deviation**
AWGN	9.74%	10.28%	9.21%	0.24%
TDL 1	9.6%	14.11%	6.18%	1.85%
TDL 2	9.7%	11.17%	8.69%	0.49%
TDL 3	9.63%	10.47%	8.69%	0.34%
$N_{Frag} = 300$				
	Mean	**Maximum**	**Minimum**	**Standard deviation**
AWGN	9.71%	10.15%	9.34%	0.2%
TDL 1	9.67%	13.33%	6.4%	1.58%
TDL 2	9.71%	11.18%	8.68%	0.39%
TDL 3	9.69%	10.60%	8.99%	0.33%

Table 22: SNR statistics for 50 simulations in DL

Where TDL 1 correspond to a channel with Doppler = 0 Hz, TDL 2 correspond to a channel with Doppler = 20 Hz y TDL 3 correspond to a channel with Doppler = 40 Hz.

So the chosen values of N_{Frag} and T_{Frag} are:

	N_{Frag}	T_{Frag}
AWGN	50	100
TDL	200	100

Table 23: Values for N_{Frag} and T_{Frag} in DL

In addition, the analysis will study the different SNRs obtained when varying, for example, the modulation and coding scheme index (IMCS), which, as seen above, takes values from IMCS=0 to IMCS=13. The simulation has been performed with an SNR sensitivity of 0.1 dB.

The bits to be sent on the channel in the transports blocks according to the downlink transport block size are defined in the following table:

I_{TBS}	I_{SF}							
	0	1	2	3	4	5	6	7
0	16	32	56	88	120	152	208	256
1	24	56	88	144	176	208	256	344
2	32	72	144	176	208	256	328	424
3	40	104	176	208	256	328	440	568
4	56	120	208	256	328	408	552	680
5	72	144	224	328	424	504	680	872
6	88	176	256	392	504	600	808	1032
7	104	224	328	472	584	680	968	1224
8	120	256	392	536	680	808	1096	1352
9	136	296	456	616	776	936	1256	1544
10	144	328	504	680	872	1032	1384	1736
11	176	376	584	776	1000	1192	1608	2024
12	208	440	680	904	1128	1352	1800	2280
13	224	488	744	1032	1256	1544	2024	2536

Figure 72: Transport Block size table for NPDSCH

In the table it can be seen that in addition to the IMCS value, they depend on the ISF value.

The channels used in these simulations would be two, the AWGN channel and the TDL channel described in previous sections.

The spectral efficiency will also be calculated, which is calculated as follows:

$$SE = \frac{Throughput}{BW} = \frac{\frac{TBS}{TTI}}{BW} \tag{28}$$

where $TTI = NSF \cdot N_{reps} \cdot T_{Subframe}$; $T_{Subframe} = 1ms$. TTI is the transmission time interval, N_{reps} is the number of repetition for each subframe, NSF is the number of subframe and, finally, TBS is determined by NSF or ISF and IMCS

In order not to have to calculate all the combinations, it has been decided to calculate for each value of the IMCS index the SNR value that fulfills the highest spectral efficiency, this would be associated to a single value of ISF.

4.4.1.1 Baseline configuration and simulation

In this simulation the most basic scenario will be studied, the SNR value for the different IMCS will be studied with the ISF that provides the best efficiency. As seen, the ISF parameter controls the number of subframes dedicated to the NPDSCH information. In this case no repetitions are used, the Doppler effect is null and the channel estimator is perfect.

IMCS	ISF/NSF	TBS	Data Rate [kbps]	Efficiency	SNR AWGN Channel [dB]	SNR TDL Channel [dB]
0	6/8	208	26.0	0.1444	-5.5	-2.7
1	3/4	144	36.0	0.2	-4	-1.3
2	2/3	144	48	0.2666	-2.8	0
3	2/3	176	58.67	0.3259	-2	0.8
4	2/3	208	69.33	0.3851	-1.2	1.6
5	7/10	872	87.2	0.4844	0.1	3
6	7/10	1032	103.2	0.5733	0.8	3.8
7	7/10	1224	122.4	0.68	1.7	4.7
8	6/8	1096	137.0	0.7611	2.2	5.3
9	6/8	1256	157.0	0.872	2.9	6
10	4/5	872	174.4	0.9688	3.5	6.5
11	7/10	2024	202.4	1.1244	4.6	7.7
12	7/10	2280	228.0	1.266	5.5	8.6
13	3/4	1032	258.0	1.4333	7.2	10.4

Table 24: Simulation of number of subframes

In this case it can be clearly seen how to maintain a BLER of 10% for a TDL channel it would be necessary to increase ≈ 3 dB, this is because the taps of the TDL channel add attenuation to the received signal, since it is a fading channel, in the case of AWGN, the channel would be flat in addition to not being a fading channel. Therefore, if the more realistic case is to be considered, this dB difference should be taken into account.

4.4.1.2 Impact of the channel estimator

In this analysis it will be studied the impact of changing the perfect channel estimator, which estimates the channel perfectly, with a more practical channel estimator, this practical estimator is the one described in the previous sections.

The following results have been obtained.

IMCS	ISF/NSF	TBS	Data Rate [kbps]	Efficiency	SNR AWGN Perfect Channel Estimator [dB]	SNR AWGN Practical Channel Estimator [dB]	SNR TDL Perfect Channel Estimator [dB]	SNR TDL Practical Channel Estimator [dB]
0	6/8	208	26	0.1444	-5.5	-2.5	-2.7	1.4
1	3/4	144	36	0.2	-4	-0.3	-1.3	2.5
2	2/3	144	48	0.2666	-2.8	0.7	0	3.6
3	2/3	176	58.67	0.3259	-2	1.3	0.8	4.3
4	2/3	208	69.33	0.3851	-1.2	1.9	1.6	4.9
5	7/10	872	87.2	0.4844	0.1	2.6	3	5.7
6	7/10	1032	103.2	0.5733	0.8	3.2	3.8	6.3
7	7/10	1224	122.4	0.68	1.7	4.1	4.7	7.2
8	6/8	1096	137	0.7611	2.2	4.6	5.3	7.6
9	6/8	1256	157	0.872	2.9	5.3	6	8.4
10	4/5	872	174.4	0.9688	3.5	5.7	6.5	8.7
11	7/10	2024	202.4	1.12444	4.6	6.9	7.7	9.9
12	7/10	2280	228	1.266	5.5	7.7	8.6	10.7
13	3/4	1032	258	1.433	7.2	9.2	10.4	12.7

Table 25: Simulation of different channel estimator

In this case when using a practical channel estimator, the difference between the SNR values obtained for a BLER of 10% for the AWGN channel and the TDL channel is approximately 3 dB. With respect to the use of a perfect channel estimator compared to a practical channel estimator, there is a perceptible difference in the SNR value. Comparing the AWGN channels with perfect estimator and without perfect estimator, it can be seen that for low IMCS values the difference is about 3.5 dB, while for higher IMCS values the difference is reduced to about 2 dB. The same comparison with the TDL channel shows that for low IMCS values a difference of about 4 dB is obtained, while for larger IMCS values the difference is 2 dB as it happened in the case of the AWGN channel.

Therefore, when the channel estimator is not perfect and it is a practical estimator, it can be seen that the dB difference is smaller when the channel uses a high IMCS.

4.4.1.3 Impact of the number of repetitions

In this analysis it will be studied the impact of modifying the number of repetitions, for this purpose the Ireps parameter is modified, which marks how many times a subframe is transmitted. The maximum number described in DL is 2048. In this case, up to 8 repetitions have been simulated.

The following results have been obtained:

TDL Channel			1 Repetition			2 Repetitions			4 Repetitions			8 Repetitions		
IMCS	ISF/NFS	TBS	SNR [dB]	Efficiency	Data Rate [kbps]	SNR [dB]	Efficiency	Data Rate [kbps]	SNR [dB]	Efficiency	Data Rate [kbps]	SNR [dB]	Efficiency	Data Rate [kbps]
0	6/8	208	-2.7	0.144	26	-5.7	0.072	13	-8.7	0.036	6.5	-11.5	0.018	3.25
4	2/3	208	1.6	0.385	69.3	-1.3	0.193	34.67	-4.4	0.096	17.33	-7.2	0.048	8.67
10	4/5	872	6.5	0.968	174.4	3.7	0.484	87.2	0.7	0.242	43.6	-2.3	0.121	21.8
13	3/4	1032	10.4	0.143	258	7.6	0.717	129	4.6	0.358	64.5	1.6	0.179	32.25

Table 27: Simulation of different number of repetitions for a TDL channel for DL scenario

AWGN Channel			1 Repetition			2 Repetitions			4 Repetitions			8 Repetitions		
IMCS	ISF/NFS	TBS	SNR AWGN Channel [dB]	Efficiency	Data Rate [kbps]	SNR [dB]	Efficiency	Data Rate [kbps]	SNR Channel [dB]	Efficiency	Data Rate [kbps]	SNR AWGN Channel [dB]	Efficiency	Data Rate [kbps]
0	6/8	208	-5.5	0.144	26	-8.2	0.072	13	-11.5	0.036	6.5	-14.6	0.018	3.25
4	2/3	208	-1.2	0.385	69.3	-4.2	0.193	34.67	-7.2	0.096	17.33	-10.3	0.048	8.67
10	4/5	872	3.5	0.968	174.4	0.5	0.484	87.2	-2.6	0.242	43.6	-5.3	0.121	21.8
13	3/4	1032	7.2	0.143	258	4.3	0.717	129	1.3	0.358	64.5	-1.7	0.179	32.25

Table 26: Simulation of different number of repetitions for a AWGN channel for DL scenario

As can be seen, doubling the number of repetitions, in both cases, for AWGN channel and TDL channel, it leads to gain a 3dB approx as increase reliability. When the number of repetitions is increased, the coverage area is also extended, but with the disadvantage of losing data rate and spectral efficiency.

4.4.1.4 Impact of the Doppler effect

The Doppler effect at the channel level means that the fragment does not take the same value, but has a certain variation, which causes the channel attenuation to be different in a fragment. This Doppler effect is considered to be studied in the case of the TDL channel, for the AWGN case it does not make sense since the channel is flat and this effect would not make sense.

In order to observe the Doppler effect it is possible to see the shape of the channel, because for a Doppler value = 0 Hz, it is almost flat, due to the fact that the transport block is a low value. By increasing the Doppler value, it generates a certain ripple in the channel, therefore, by observing in the channel that the Doppler effect generates this ripple, it is possible to check if the perfect channel estimator can estimate and correct this undulation.

Several tests have been performed and it is verified that the perfect estimator is able to estimate these small channel ripples due to the Doppler effect, the perfect channel estimator corrects any Doppler value. It can be appreciated both in the ripples it generates in the channel (graphically) and in the values obtained for a given SNR, which are close to the values of a simulation with zero Doppler and would be within the margin of error of the simulation. This can be visualized in the following pictures:

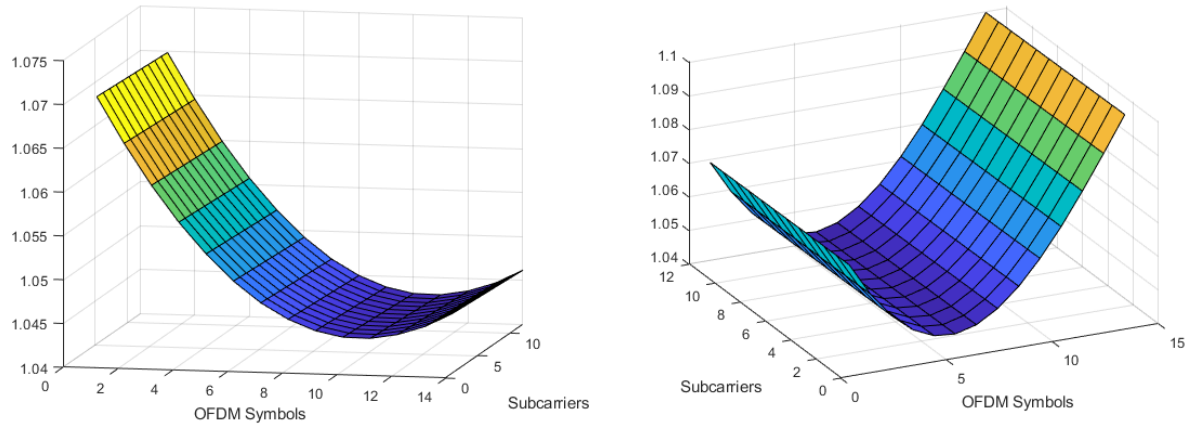

(a) (b)

Figure 73: Perfect channel estimator grid with a Doppler=100Hz (a) Perfect channel estimator grid with a Doppler=200Hz (b)

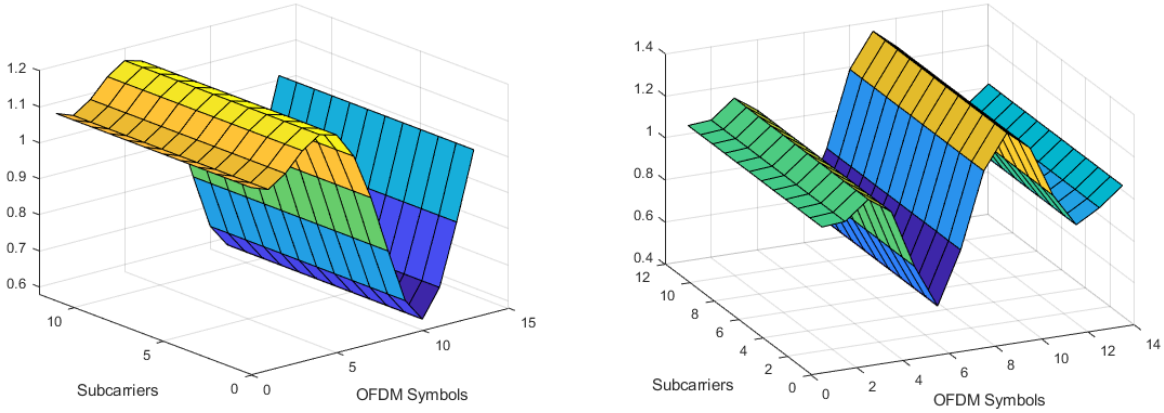

(a) (b)

Figure 74: Perfect channel estimator grid with a Doppler=1kHz (a) Perfect channel estimator grid with a Doppler=2kHz (b)

Therefore, it does not make sense to look at the impact of Doppler in this type of scenario, because the channel will not have that wavelet variability, it would only have the noise variability.

On the other hand, it would still be necessary to test the practical channel estimator, this estimator should have more wavelet variability. But for the practical channel estimator, the same behavior is observed, it does not estimate exactly the same channel, but it can estimate approximately these waves, it can be viewed graphically as the estimator tries to correct this variability.

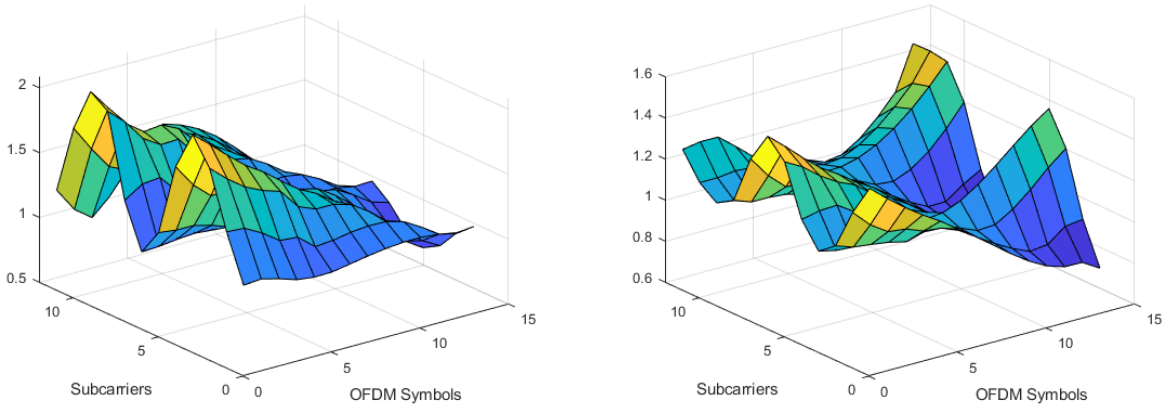

(a) (b)

Figure 75: Practical channel estimator grid with a Doppler=100Hz (a) Practical channel estimator grid with a Doppler=200Hz (b)

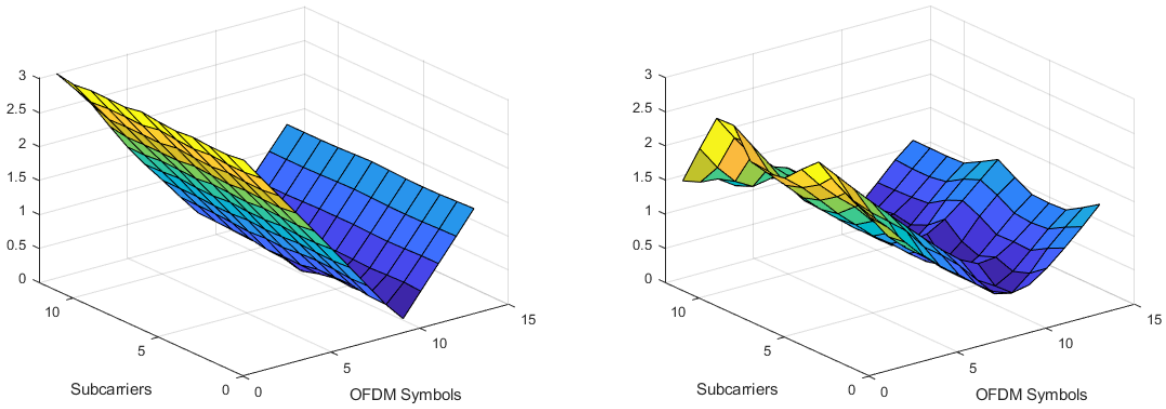

(a) (b)

Figure 76: Practical channel estimator grid with a Doppler=1kHz (a) Practical channel estimator grid with a Doppler=2kHz (b)

But a more rigorous way to know if the practical estimator is able to correct this Doppler effect would be to perform simulations. Different simulations have been performed in order to obtain conclusive results. In this section it has been considered that the maximum Doppler error can be about 40 Hz, obtaining the following results.

Practical Channel Estimator			
IMCS / ISF	SNR Doppler = 0 Hz [dB]	SNR Doppler = 40 Hz [dB]	SNR Doppler = 100 Hz [dB]
0 / 6	1.4	0.9	1.8
1 / 3	2.5	2.7	1.8
10 / 4	8.7	9	8.2
13 / 3	12.7	13.6	14.8

Table 28: SNR using different values of Doppler for a practical channel estimator

It can be seen that for a Doppler effect of 40Hz, the practical channel estimator is able to correct it, since we would obtain values that would be within the dispersion of the SNR value for a BLER of 10%.

To verify that the practical estimator is not able to correct higher Doppler values, the following checks have been performed.

For each value of IMCS / ISF the simulation has been performed for a different Doppler, because if the value of IMCS / ISF is very large and the Doppler is very strong, the system is not able to obtain a BLER of 10% even for very high SNR values (around 30 dB).

This effect can also be observed in the previous figures, it can be appreciated that when the Doppler effect is very strong, the practical estimator is not able to estimate these channel wavelets.

Practical Channel Estimator	
IMCS / ISF	SNR Doppler Variable depends on IMCS [dB]
1 / 3	9.4 (Doppler = 1 kHz)
10 / 4	16.1 (Doppler = 700 kHz)
13 / 3	17.5 (Doppler = 400 kHz)

Table 29: SNR using high values of Doppler for a practical channel estimator

Depending on the Doppler value and the chosen IMCS, the system is not able to obtain a BLER of 10%, neither for very high SNR values, so for each IMCS tests have been performed at different Doppler values, some at 400Hz, 600Hz or even 1kHz.

It can be concluded that with these estimators, it is not possible to obtain the impact of the Doppler error.

4.4.2 NB-IoT NPUSCH performance

In this case, the case of uplink system performance will now be considered by performing NPUSCH simulations.

The idea is the same as in the NPDSCH case, the simulations will be split into two variables, T_{Frag} and N_{Frag}, being the fragment duration and the number of fragments respectively.

The intention is similar, to obtain a BLER standard of 10% for the system to operate correctly and to calculate the number of simulations to obtain a BLER standard dispersion of less than 3% for a fixed value of SNR and therefore also to characterize the behavior of the Rice variable.

As indicated above, the values of N_{Frag} and T_{Frag}have been chosen to be the same values as in the DL scenario, and to fulfill a dispersion of less than 3%.

For each scenario, 50 simulations have been simulated in order to correctly characterize the scenario and extract the corresponding statistics. For this computation, only the case where MT=12 subcarriers and SCS=15kHz has been taken into account. The SNR value fixed for both studies is $SNR = -3.7dB$.

The statistics to be taken into account are:

- BLER average
- Maximum BLER
- Minimum BLER
- Standard deviation, it will be computed using the following formula, with N=50.

$$\sigma = \sqrt{\frac{\sum_{i=1}^{n}(x_i - \bar{x})^2}{N}} \tag{29}$$

The results are the following:

$N_{Frag} = 50$				
	Mean	**Maximum**	**Minimum**	**Standard deviation**
AWGN	8.76%	9.66%	7.64%	0.44%
TDL	33.73%	44.24%	22.42%	5.46%
$N_{Frag} = 100$				
	Mean	**Maximum**	**Minimum**	**Standard deviation**
AWGN	8.77%	9.55%	8.33%	0.29%
TDL	33.79%	41.16%	25.83%	3.80%
$N_{Frag} = 200$				
	Mean	**Maximum**	**Minimum**	**Standard deviation**
AWGN	8.76%	9.13%	8.36%	0.18%
TDL	33.48%	39.90%	27.92%	2.76%
$N_{Frag} = 300$				
	Mean	**Maximum**	**Minimum**	**Standard deviation**
AWGN	8.77%	9.11%	8.42%	0.16%
TDL	33.60%	38.25%	28.59%	2.18%

Table 30: SNR statistics for 50 simulations in UL

So the chosen values of N_{Frag} and T_{Frag} are:

	N_{Frag}	T_{Frag}
AWGN	50	100
TDL	200	100

Table 31: Values for N_{Frag} and T_{Frag} in UL

For the remaining analysis, other configurations are also considered, such as changing the MT value to 6 or 3 or the ST value to 1 subcarrier. In addition, the case where the SCS is varied to 3.75 kHz will be studied.

All simulations have been performed with an SNR sensitivity of 0.1 dB.

In the case of the UL scenario, The bits to be sent on the channel in the transports blocks according to the uplink transport block size are defined in the following table:

I_{TBS}	I_{RU}							
	0	1	2	3	4	5	6	7
0	16	32	56	88	120	152	208	256
1	24	56	88	144	176	208	256	344
2	32	72	144	176	208	256	328	424
3	40	104	176	208	256	328	440	568
4	56	120	208	256	328	408	552	680
5	72	144	224	328	424	504	680	872
6	88	176	256	392	504	600	808	1000
7	104	224	328	472	584	712	1000	1224
8	120	256	392	536	680	808	1096	1384
9	136	296	456	616	776	936	1256	1544
10	144	328	504	680	872	1000	1384	1736
11	176	376	584	776	1000	1192	1608	2024
12	208	440	680	1000	1128	1352	1800	2280
13	224	488	744	1128	1256	1544	2024	2536

Figure 77: Transport Block size table for NPUSCH

The table shows that in addition to the IMCS value, it also depends on the value of the index I_{RU}, which is related to the number of resource unit, N_{RU}, this relationship was explained in previous sections.

The channels used in these simulations would be two, the AWGN channel and the TDL channel.

In the uplink case, the spectral efficiency can be calculated as follows:

$$SE = \frac{Throughput}{BW} = \frac{\frac{TBS}{TTI}}{BW} \tag{30}$$

where $TTI = N_{RU} \cdot T_{RU}$.

TTI is the transmission time interval, N_{RU} is the number of resource unit transmitted and T_{RU} is the time it takes to transmit one RU, it change depending on the value of MT/ST. Finally, TBS is determined by N_{RU} or I_{RU} and IMCS. The bandwidth depends on the mode of operation, MT or ST. Therefore the bandwidth would be 180 kHz (MT=12), 90 kHz (MT=6), 45kHz (MT=3) , 15kHz (ST=1, SCS = 15kHz), 3.75 kHz (ST=1, SCS = 3.75kHz)

In order not to have to calculate all combinations, it has been decided to calculate for several values of the IMCS index the SNR value that satisfies the highest spectral efficiency, which would be associated with a single value of N_{RU} according to the previous table.

4.4.2.1 Baseline configuration and simulation

In this section it will be analyzed the study of a base scenario, the SNR value will be studied for different IMCS and RU to obtain the best efficiency. In this case, no repetitions have been used, the Doppler effect is null and the channel estimator is perfect.

The study will be performed for different configurations of contiguous subcarriers within a RU. There are 1,3,6 or 12 continuous subcarriers for NPUSCH for the case where the

SCS is 15 kHz.

The study will also be performed for SCS = 3.75 kHz, in this case the number of continuous subcarriers is equal to 1.

All simulations are presented in the tables below:

MT=12 - SCS=15kHz						
IMCS	I_{RU}/N_{RU}	**TBS**	**Data Rate [kbps]**	**Efficiency**	**SNR AWGN Channel [dB]**	**SNR TDL Channel [dB]**
0	6/8	208	26	0.145	-5.7	-2.4
4	2/3	208	69.34	0.385	-1.4	1.8
10	4/5	872	174.4	0.969	3.2	6.8
12	3/4	1000	250	1.389	6.8	10.3

Table 32: Baseline simulation for MT=12 subcarriers and SCS=15 kHz

MT=6 - SCS=15kHz						
IMCS	I_{RU}/N_{RU}	**TBS**	**Data Rate [kbps]**	**Efficiency**	**SNR AWGN Channel [dB]**	**SNR TDL Channel [dB]**
0	6/8	208	13	0.145	-5.8	-2.4
4	2/3	208	34.67	0.385	-1.4	1.7
10	4/5	872	87.2	0.969	3.2	6.8
12	3/4	1000	125	1.389	6.8	10.3

Table 33: Baseline simulation for MT=6 subcarriers and SCS=15 kHz

MT=3 - SCS=15Hz						
IMCS	I_{RU}/N_{RU}	**TBS**	**Data Rate [kbps]**	**Efficiency**	**SNR AWGN Channel [dB]**	**SNR TDL Channel [dB]**
0	6/8	208	6.5	0.145	-5.7	-2.4
4	2/3	208	17.34	0.385	-1.4	1.9
10	4/5	872	43.6	0.969	3.2	6.8
12	3/4	1000	62.5	1.389	6.8	10.3

Table 34: Baseline simulation for MT=3 subcarriers and SCS=15 kHz

ST=1 - SCS=15Hz						
IMCS	I_{RU}/N_{RU}	**TBS**	**Data Rate [kbps]**	**Efficiency**	**SNR AWGN Channel [dB]**	**SNR TDL Channel [dB]**
0	6/8	208	3.25	0.2167	-4	-0.6
4	2/3	208	8.67	0.578	0.6	3.9
10	4/5	872	21.8	1.453	7.9	11.3

Table 35: Baseline simulation for ST=1 subcarriers and SCS=15 kHz

ST=1 - SCS=3.75Hz						
IMCS	I_{RU}/N_{RU}	**TBS**	**Data Rate [kbps]**	**Efficiency**	**SNR AWGN Channel [dB]**	**SNR TDL Channel [dB]**
0	6/8	208	0.8125	0.2167	-4	-0.7
4	2/3	208	2.167	0.578	0.6	3.9
10	4/5	872	5.45	1.453	7.8	11.3

Table 36: Baseline simulation for ST=1 subcarriers and SCS=3.75 kHz

Initially, it can be observed that the difference between the performance of the AWGN channel and the TDL channel is $\approx$ 3dB, as in the case of DL.

Notice that for the MT = 12, 6 and 3 cases, almost the same SNR values are obtained, this is because although the number of tones varies, the number of slots also varies, being nSlot = 2, 4 and 8 respectively. This means that the amount of information sent is the same. The difference is seen when using ST=1, where the number of slots is equal to 16. This means that the SNR value must increase in order to receive all the information correctly for the same IMCS and N_{RU} compared to the multi-tone case. On the negative side, the SNR deteriorates $\approx$ 2 dB for low IMCS values and $\approx$ 4.5 dB for high IMCS values.

It is important to note that the case of IMCS = 12 has not been studied for the ST=1 cases, since the software does not allow this scenario.

Note that as the number of carriers decreases, the T_{RU} increases, so the throughput reduces but spectral efficiency is maintained, note that the spectral efficiency remains constant for modes MT = 12, 6 and 3, since the T_{RU} changes and the BW also changes and the final value is compensate between them. The worst data rate is for ST=1 and SCS=3.75 kHz, where the T_{RU} is 32 ms. Emphasize that for ST=1 with SCS =3.75 kHz or 15 kHz, the spectral efficiency has improved.

4.4.2.2 Impact of the channel estimator

The results of both estimators, the perfect channel estimator and the practical estimator, are shown in the following table.

IMCS	I_{RU}/N_{RU}	TBS	Data Rate [kbps]	Efficiency	SNR AWGN Channel [dB]	SNR TDL Channel [dB]
0	0/1	16	16	0.0889	-2.8	-0.8
7	0/1	104	104	0.5778	1.9	4.6
13	0/1	224	224	1.244	7.2	10.1

Table 37: Simulation of different channel estimator

The use of a practical channel instead of a perfect channel is a necessary simulation, since the perfect channel estimator would not be the real case. So it is remarkable, since it worsens the received SNR by 3 dB for high IMCS values and 2 dB for low IMCS values.

When designing the system, the estimator used and its performance must be taken into account.

4.4.2.3 Impact of the number of repetitions

In this section it is studied how the system would behave if the number of repetitions variable is increased, this variable, as in the previous case, measures how many times the same information is repeated. It leads to a loss of efficiency and a decrease in data rate each time the transmissions are doubled. Up to 8 repetitions have been simulated. The following results were obtained:

AWGN Channel			1 Repetition			2 Repetitions			4 Repetitions			8 Repetitions		
IMCS	I_{RU}/N_{RU}	TBS	SNR AWGN Channel [dB]	Efficiency	Data Rate [kbps]	SNR AWGN Channel [dB]	Efficiency	Data Rate [kbps]	SNR AWGN Channel [dB]	Efficiency	Data Rate [kbps]	SNR AWGN Channel [dB]	Efficiency	Data Rate [kbps]
0	0/1	16	-3.8	0.0889	16	-6.7	0.0445	8	-9.8	0.0223	4	-12.8	0.0112	2
7	0/1	104	1.4	0.5778	104	-2	0.2889	52	-5.1	0.1445	26	-8	0.0722	13
13	0/1	224	6.8	1.2444	224	1	0.6222	112	-2	0.3111	56	-5	0.1556	28

Table 38: Simulation of different number of repetitions for a AWGN channel for UL scenario

TDL Channel			1 Repetition			2 Repetitions			4 Repetitions			8 Repetitions		
IMCS	I_{RU}/N_{RU}	TBS	SNR TDL Channel [dB]	Efficiency	Data Rate [kbps]	SNR TDL Channel [dB]	Efficiency	Data Rate [kbps]	SNR TDL Channel [dB]	Efficiency	Data Rate [kbps]	SNR TDL Channel [dB]	Efficiency	Data Rate [kbps]
0	0/1	16	-1.2	0.0889	16	-4.2	0.0445	8	-7.2	0.0223	4	-10.2	0.0112	2
7	0/1	104	4.3	0.5778	104	1	0.2889	52	-2.1	0.1445	26	-5.1	0.0722	13
13	0/1	224	9.7	1.2444	224	4.1	0.6222	112	1.1	0.3111	56	-1.9	0.1556	28

Table 39: Simulation of different number of repetitions for a TDL channel for UL scenario

In the two channels, it is observed that the increase in the number of repetitions, leads to an improvement of 3 dB, this materializes in that it increases the coverage of the beam. Although half the efficiency and data rate is lost every time the information is duplicated.

It should be noted that for the transition from 1 to 2 repetitions in both channels and for high IMCS, the increase is 6 dB instead of 3 dB.

4.4.2.4 Impact of the doppler effect

An important aspect to study is how Doppler affects the performance of the received signal. In the DL case, the two estimators corrected perfectly the low Doppler values, but it is interesting to check it in the uplink case since the modulation and channel coding is different in UL and may vary the simulations. All this has been done for the case MT=12 and SCS=15 kHz.

MT = 12 - SCS= 15kHz - TDL Channel				
IMCS / N_{RU}	SNR Doppler = 0 Hz [dB]	SNR Doppler = 40 Hz [dB]	SNR Doppler = 100 Hz [dB]	SNR Doppler Variable depends on IMCS [dB]
0 / 1	-0.8	-0.3	-0.3	2.5 (Doppler = 1 kHz)
7 / 1	4.6	5.2	5.2	6.7 (Doppler = 600 Hz)
13 / 1	10.1	10.7	10.9	13.7 (Doppler = 300 Hz)

Table 40: Simulation of different number of Doppler for a TDL channel for UL scenario

In order to characterize approximately the whole IMCS table, three values of IMCS have been simulated, one low, one high and one medium.

It is observed that the values for a Doppler $\leq$ 100, the values are within the dispersion range, so that the practical estimator also corrects in this case the Doppler effect.

In addition, a last column has been added to verify that for very high Doppler values, the estimator is not able to correct it. For each value of IMCS / N_{RU} the simulation has been performed for a different Doppler, because if the value of IMCS / N_{RU} is very high and the Doppler is very large, the system is not able to obtain a BLER 10% even for very high SNR values (around 30-35 dB).

5 Conclusions and future development:

In this study, the NB-IoT NTN scenario has been characterized by creating a program from scratch. In this program it is possible to obtain from some inputs, such as NTN parameters, (e.g. the spherical geometry of the earth, the parameters associated with the satellite, such as orbit or speed), the antenna parameterization, (which allows using any type of antenna) or the link budget parameters (e.g. transmission power, frequency, pathloss), it is possible to obtain a global characterization of the scenario, obtaining outputs like the characterization of the satellite footprint coverage (e.g. with heatmap representations or SNR statistics and its CDF), the characterization of the beam pointing, for any given angle, or the characterization of the satellite pass (e.g. characterizing the evolution of the SNR), the characterization of the beam pointing, for any given angle, or the characterization of the satellite pass (e.g. characterizing the SNR evolution, the Doppler effect or the propagation delay).

This program offers an enormous degree of freedom, since it is possible to modify any input and obtain different scenarios and different results. It is possible to characterize another type of satellite, for example GEO, it is feasible to change the type of antenna, for example, a vendor can indicate the radiation pattern of its antenna in terms of theta or phi, or in terms of azimuth and elevation and can be incorporated into the program for performance analysis and characterize it in NB-IoT NTN communications.

The main conclusions are as follows; it should be emphasized that these conclusions are observations based on the particular scenario considered and may vary depending on the different scenarios.

- Static study
  - One beam

    The DL case is limited in power, especially at the edges of the beam, while the UL case has a better performance, because the bandwidth used is narrower and the noise does not affect as much as in DL. The difference between the DL case and the UL case is about 9 dB. With this improvement, the UL case improves the coverage area up to 9 times more than the DL case.

    When the antenna tilt is modified, the pointing area is improved, but it is observed that the area at -10 dB is the same as when pointing at Nadir, although the SNR values would no already be so high, since by changing the pointing, the distance between satellite and UE increases. In the case of UL, it does increase the area a bit at 0 dB with respect to pointing at Nadir.

  - Multiple beam

    In the case of two antennas, therefore two beams, it is obvious that the coverage is improved, if it is compared with the case of one beam, in the DL case it is observed that the area is approximately doubled for all SNR ranges. In the UL case the same does not occur, only the range is doubled for high SNR, when the SNR range is low, the coverage area is practically the same.

- Dynamic study
  - Variation of SNR in terms of elevation angle

    The SNR variation between different elevation angles is about 12 dB, so depending on where a device is located its performance can be significantly degraded.

  - Doppler shift and Doppler shift rate

    The maximum Doppler shift value occurs when the satellite is flying away from the UE. The maximum value is ± 46kHz for a carrier frequency pf 2 GHz.

    The maximum Doppler shift rate occurs when the satellite is flying over the device. This value depends on the elevation angle. For $\alpha = 90$, the maximum value is 1021 Hz/s, for $\alpha = 45$, the maximum value is -747.4 Hz/s and for $\alpha = 30$ the maximum value is -564.2 Hz/s. It can be seen that the difference is $\approx$ 450 Hz/s between $\alpha = 90$ and $\alpha = 30$.

  - Delay propagation and delay propagation rate

    The maximum value of propagation delay is 10ms and occurs when the satellite is far away from the device. When the satellite is flying above the UE, this delay depends on the elevation angle. For $\alpha = 90$, the maximum value is 1.8 ms, for $\alpha = 45$, the maximum value is 2.5 ms and for $\alpha = 30$ the maximum value is 3.3 ms. This implies a delay difference of 1.4 ms between $\alpha = 90$ and $\alpha = 30$.

    The maximum value of propagation delay rate is 36 $\mu s/s$ and it is when the satellite is flying away from the user.

The conclusions main of the second part would be the following:

- NPDSCH Block Error Rate Simulation

  Starting from the baseline, the SNR range for the total IMCS set using the AWGN channel is [-5.5 dB to 7.2 dB], while for the TDL channel the range is [-2.7 dB to 10.4 dB], which is an increase of 3dB between the two channels.

  If it is considered that the channel estimator is not perfect and the one described in previous sections is used, the SRN range using an AWGN channel is [-2.5 dB to 9.2 dB] while using a TDL channel is [1.4 dB to 12.7 dB]. In the AWGN channel the difference is 3.5 dB for low IMCS values and 4 dB for high values. While in the TDL channel the difference is 4 dB for low IMCS values and 2 dB for high values.

  The number of repetitions also implies an improvement in both channels. This improvement is 3 dB each time the transmissions are duplicated, thus improving the SNR value since the same information is sent several times but it loses rate and spectral efficiency.

  The Doppler error is corrected with the estimators that have been considered in the study, so it is not possible to see how the SNR value differs.

- NPUSCH Block Error Rate Simulation

In this case it can be seen as for MT=12, MT=6 and MT=3 approximately the same values are obtained, for the AWGN channel a SNR range of [-5.7 dB to 6.8 dB] is obtained and for the TDL channel a range of [-2.4 dB to 10.3 dB] is obtained. Thus, it can be seen that the difference between using one channel or the other is 3dB.

For the case of ST=1 using SCS=15kHz and ST=1 using SCS=3.75kHz the range is practically the same for both cases. For the AWGN channel the SNR range is [-4 dB to 7.8 dB] and the SNR range in the TDL channel is [-0.7 dB to 11.3 dB]. In these last two cases, compared to the previous ones, the SNR worsens about 2 dB for low IMCS values and worsens 4 dB for high values.

On the other hand, the channel estimator, it is observed that it worsens 3 dB for high values of IMCS and 2 dB for low values of IMCS. The AWGN channel has an SNR range of [-2.8 dB to 7.2 dB] while the TDL channel has an SNR range of [-0.8 dB to 10.1 dB].

For the number of repetitions, it is observed that with each increase, there is an increase of 3 dB. It should be noted that for high IMCS values, both for AWGN and TDL, the improvement is approximately 6 dB when increasing from 1 repetition to 2 repetitions.

To conclude the study, it has been seen convenient to collect all the data in order to see if it is feasible to use NB-IoT devices in communications with LEO satellites.

It has been divided into two parts, one for DL and one for UL.

For the DL case the performance is lower since the maximum SNR value that reaches the Earth's surface and gives coverage is - 3dB. Therefore, for the baseline case, low IMCS values could be used and the devices would have coverage both in AWGN channel and TDL channel, if the estimator is changed, with the TDL channel it would not be possible since the minimum value needed is 1.4 dB. If the number of repetitions is increased, it is observed that for 8 repetitions it is possible to use the whole range of IMCS for the AWGN channel, while for the TDL channel it would be possible to use lower values of IMCS ($IMCS \leq 10$).

Therefore, to obtain a wide range of coverage, $SNR \geq -10(dB)$, several repetitions should be used, since it would increase 3 dB each time the value is doubled, and it would compensate the losses of the estimator and the losses of the TDL channel in reference to the AWGN, in addition to using low IMCS values.

In the case of uplink, the performance is better, for the basic scenario, both channels can be used, since the maximum SNR value that has coverage is approximately 6 dB, if low or medium IMCS values are used. This is valid for MT or ST. Changing to a practical channel estimator, it could also be possible to continue to use the devices, with a low and medium IMCS value.

If the number of repetitions is increased, for the AWGN channel with 2 repetitions the whole IMCS range can be used, and for the TDL channel the same is valid, for 2 repetitions the whole IMCS range is possible.

Therefore, in order to use NB-IoT devices in UL within a $SNR \geq -10(dB)$ area, if the devices use a number of repeats greater than or equal to 2, any combination of IMCS could be used to communicate, both for the AWGN channel and for the TDL channel.

For future research, it would be interesting to characterize more NB-IoT scenarios with the program, for other types of satellites, other types of antennas, etc... To analyse the different performances obtained. In addition, link budget analysis could be performed with different antennas to observe the different performances that could be obtained.

For future development, the capabilities of the system could be further studied, such as how many NB-IoT users could be served with the same beam.

Furthermore, the same scenarios could be simulated with different channel estimators, in order to see the effect of Doppler error.

Glossary

3GPP 3rd Generation Partnership Project

ACK Acknowledgement

AWGN Additive White Gaussian Noise

BCCH Broadcast Control Channel

BLER Block Error Rate

BPSK Binary Phase-shift keying

BW Bandwidth

CDF Cumulative distribution function

CIoT Cellular Internet of Things

CRC Cyclic Redundancy Check

DL Downlink

DMRS Demodulation Reference Signal

DRS Digital Reference Signal

eDRX extended Discontinuous Reception

EIRP Effective Isotropic Radiated Power

eMTC extended Machine Type Communications

eNB evolved Node B

GEO Geostationary Orbit

GNSS Global Navigation Satellite System

GSM Global System for Mobiles

HPBW Half Power Beam Width

ICI Inter-Carrier Interference

LEO Low-Earth Orbit

LSE Least Squares Estimation

LOS Line of Sight

LPWAN Low-Power Wide Area Network

LTE Long Term Evolution

MCS Modulation and Coding Scheme

MIB Master Information Block

mMTC Massive Machine-Type Communication

MT Multiple tones

NACK Non-Acknowledgement

NB-IoT Narrowband Internet of Things

NF Noise Figure

NGSO Non-Geostationary Satellite Orbit

NLOS Non-Line of Sight

NPBCH Physical Broadcast Channel

NPDSCH Narrowband Physical Downlink Shared Channel

NPUSCH Narrowband Physical Uplink Shared Channel

NPRACH Narrowband Physical Random Access Channel

NPSS Narrowband Primary Synchronization Signal

NSSS Narrowband Secundary Synchronization Signal

NR New Radio

NRS Narrowband Reference Signal

NRS Narrowband Reference Signal

NTN Non Terrestrial Networks

OFDMA Orthogonal Frequency Division Multiple Access

PA Pilot Aided

PDF Probability Density Function

PRB Physical Resource Block

QoS Quality of Service

QPSK Quadrature Phase Shift Keying

RA Random Access

RE Resource Element

RF Radio Frequency

RU Resource Unit

SC-FDMA Single-Carrier Frequency Division Multiple Access

SCS Subcarrier Spacing

SIB1-NB System Information Block 1 - Narrowband

SNR Signal to Noise Ratio

ST Single Tone

TA Tracking Area

TBS Transport Block Size

TDL Tapped Delay Line

UE User Device

UL Uplink

References

[1] Matthieu Kanj, Vincent Savaux, Mathieu Le Guen, "A Tutorial on NB-IoT Physical Layer Design" *IEEE Communications Surveys Tutorials*, vol. 22, no. 4, pp. 2408–2446, 2020, doi: 10.1109/COMST.2020.3022751.

[2] M. Guadalupia, J. Ferrera, R. Ferrús, I. Llorensa, A. Gonzálezc, A. Mañeroc, R. Brandborgd, H. Kroghd, A. Calverasb, T. Kellermanne, S. Afaquie, "Designing a 3GPP NB-IoT NTN service for CubeSats in low density Constellations" *72nd International Astronautical Congress (IAC)*, 25-29 October 2021.

[3] Rene Brandborg Sørensen, Henrik Krogh Møller, Per Koch, "5G NB-IoT via low density LEO Constellations" *35th Annual Small Satellite Conference*, 2021.

[4] Oltjon Kodheli, Nicola Maturo, Stefano Andrenacci, Symeon Chatzinotas, and Frank Zimmer "Link budget analysis for satellite-based narrowband IoT systems" *18th International Conference on Ad Hoc Networks and Wireless (AdHoc-Now 2019)*, Luxembourg, 1-3 October 2019.

[5] Sylvain Cluzel, Laurent Franck, Jose Radzik, Sonia Cazalens, Mathieu Dervin, Cedric Baudoin and Daniela Dragomirescu, "3GPP NB-IoT coverage extension using LEO satellites" *978-1-5386-6355-4/18/31.00 IEEE*, 2018.

[6] Matteo Conti, Stefano Andrenacci, Nicola Maturo, Symeon Chatzinotas and Alessandro Vanelli-Coralli, "Doppler Impact Analysis for NB-IoT and Satellite Systems Integration" *978-1-7281-5089-5/20/31.00 IEEE*, 2020.

[7] Dr. Gilles Charbit, Dr. Debby Lin, Dr. Kader Medles, Linda Li, and Dr. I-Kang Fu, "Space-Terrestrial Radio Network Integration for IoT" *978-1-7281-6047-4/20/31.00 IEEE*, 2020.

[8] Matteo Conti, Alessandro Guidotti, Carla Amatetti, and Alessandro Vanelli-Coralli, "NB-IoT in Non-Terrestrial Networks: Link Budget Analysis" *GLOBECOM 2020 - 2020 IEEE Global Communications Conference, 2020, pp. 1-6*, 2020.

[9] Houcine Chougrani, Steven Kisseleff, Member, Wallace A. Martins, Senior Member, and Symeon Chatzinotas, "NB-IoT Random Access for Non-Terrestrial Networks" , 29 Sep 2021.

[10] Oltjon Kodheli, Stefano Andrenacci, Nicola Maturo, Symeon Chatzinotas, Frank Zimmer, "Resource Allocation Approach for Differential Doppler Reduction in NB-IoT over LEO Satellite" *9th Advanced Satellite Multimedia Systems Conference and the 15th Signal Processing for Space Communications Workshop (ASMS/SPSC)*, 2018.

[11] Pau Tanyà I Vinyeta, Ramon Ferrús, "Performance Assessment of NB-IoT Protocol Over Satellite Channels" , Barcelona, June 2021.

[12] 3GPP TR 36.763 V1.0.0, "Study on Narrow-Band Internet of Things (NB-IoT) / enhanced Machine Type Communication (eMTC) support for Non-Terrestrial Networks (NTN) (Release 17)" , May 2021.

[13] 3GPP TR 38.811 v15.4.0, "Study on New Radio (NR) to support no-terrestrial networks (Release 15)" , Sep. 2021.

[14] 3GPP TS 36.213 v16.4.0, "Evolved Universal Terrestrial Radio Access (E-UTRA); Physical layer procedures (Release 16)" , Dec. 2020.

[15] 3GPP TS 36.211 version 14.2.0, "Evolved Universal Terrestrial Radio Access (E-UTRA); Physical channels and modulation (Release 14) " , Dec. 2020.

[16] 3GPP TR 38.901 v16.1.0, "Study on Channel model for frequencies from 0.5 to 100GHz (Release 16)" , Dec. 2019.

[17] J. Schlienz, D. Raddino, "Narrowband Internet of Things " *Whitepaper Rohde & Schwarz.*

[18] Hassan Malik, Haris Pervaiz, Muhammad Mahtab Alam, Yannick Le Moullec, Alar Kuusik and Muhammad Ali Imran, "Radio Resource Management Scheme in NB-IoT Systems" *29 March 2018.*

[19] Andreas Philipp Matz , Jose-Angel Fernandez-Prieto, Joaquin Cañada-Bago and Ulrich Birkel, "A Systematic Analysis of Narrowband IoT Quality of Service" *14 March 2020.*

[20] Cesar Benavente and Ramon Garcia"NUEVAS IMPLEMENTACIONES DIGITALES DE SINCRONISMOS DE BIT Y PORTADORA EN MODEM CPM" *Madrid 1999.*